Syntheses and photophysico-chemical properties of phthalocyaninesin the presence of silica nanoparticles.

A thesis submitted in fulfilment of the requirement of the degree of

Masters Degree of Science

At

Rhodes University

By

Siwaphiwe Peteni

March 2018

Acknowledgements

My utmost appreciation goes to the Dist. Professor Tebello Nyokong, for allowing me to work under her wing and the opportunities she has afforded me ~Thank you

To my Japan hosts Professor Kobayashi and Mutsumuyi , I am very much grateful for hosting us for two months, for giving us ideas for our work and for showing us places in Japan ~ Arigatogozaimashita. To my co-supevisor Dr.Britton and Dr Mack~ Thank you. To my mother Bulelwa Peteni, your prayers throughout my Masters course have not gone unheard~ EnkosiMagudu. To Gail, the Boss lady, ons is baiedankbaarvil al u werk ~baiedankie and Papa Francis ~ Wazviita

To Drs.Sekhosane, OLuwole “bhutiza” and Babu, thank you very much helping out with the running my experiments, and for being patient with me. To my S22 lab mates, you made my masters journey enjoyable, the jokes, the singing and dancing around the lab aaahh thanks you guys ~smiles~. To the chemical Michael Jackson Nwaji, thank you for helping out with some ideas and synthesis for my work, enkosi my leader. To the former and present lab managers, your work has not gone unnoticed, ons is baiedaankbaar. To my siblingsZandile,Avela and Lundi, Nqabakazi, Simamkelendiyanithanda. Cousins Dumentlango, Aphiwe, Luphiwe for harassing me to take it easy with school ~smiles~ ndiyabulelabantasendiyanithanda. To my friends, thank you for the support ~XOXO.

Financial support from National research fund, Innovation, scarce skills and development scholarship, South Africa is greatly acknowledged.

To God be the Glory!!!!!

Abstract

This thesis reports on the syntheses and characterizationof symmetrical (charged and neutral), asymmetrical (neutral) metallophthalocyanines (MPcs) and subphthalocyanines (SubPcs). The charged and neutral Pcs were physically doped onto silica nanoparticles (SiNPs). The asymmetrical MPc was also chemically linked to SiNPs. Spectroscopic and microscopic techniques were used to confirm the formation of SiNPs-MPc conjugates.

The photophysics and photochemistry of the MPcs were assessed when alone and in conjugates (with SiNPs). The studies showed no significant changes in fluorescence quantum yields (ϕ_F) and fluorescence lifetimes (ϕ_F) of MPcs following doping except for **2**-SiNPs (**2** = Zn tetraaminophenoxyphthalocyanines) and **6**-SiNPs (doped) (**6** = Zn tris[(4-(pyridine-4-ylthio)2-thio-4-methylthiazol-5yl) acetic acid phthalocyanine) where there was a decrease in the ϕ_F value. Also for **1**-SiNPs (**1** = unsubstituted ZnPc) there was an elongation in τ_F which could be due to the protection offered by SiNPs. Both charged/neutral MPcs displayed high triplet quantum yields (ϕ_T) and singlet quantum yields (ϕ_Δ) following doping except for **2**-SiNPs where there was a decrease in the latter. For **1**-SiNPs there was an increase in ϕ_T but a decrease inϕ_Δ .There wasa decrease in ϕ_T and an increase in $\phi_\Delta$for**4**-SiNPs (**4** = Zn tetrasulfophenoxyphthalocyanine), the decrease in ϕ_T could be due to the orientation of theMPc in SiNPs. An increase in both ϕ_T and ϕ_Δ for **6**-SiNPs (linked) compared to **6**-SiNPs (doped) was observed. Complex **5** (**5** = Zn tetra-kis-(dodecylmercapto) phthalocyanine) showed a low ϕ_Δ value.

Table of contents

Table of contents

List of abbreviations

^{1}HNMR	Proton Nuclear Magnetic Resonance
ADMA	Tetrasodium α,α-(anthracene-9,10-diyl) dimethylmalonate
APTES	3-Aminopropyltriethoxysilane
BET	Brunauer-Emmett-Teller
DBU	1,8-Diazabicyclo-[5.4.0]-undec-7-ene
DCC	Dicyclohexylcarbodiimide
DMAP	Dimethylaminopyridine
DMF	Dimethyl Formamide
DMSO	Dimethyl Sulfoxide
DMSO-d_6	Deuterated Dimethylsulfoxide
DPBF	1,3-Diphenylisobenzofuran
EDX	Energy-Dispersive X-ray spectroscopy
ET	Energy transfer
F	Fluorescence
FTIR	Fourier Transform Infrared
HOMO	Highest Occupied Molecular Orbital
IC	Internal conversion
ISC	Intersystem crossing
LCAO	Linear Combination of Atomic Orbitals
LUMO	Lowest Occupied Molecular Orbital
MPcs/ Pcs	Metallophthalocyanines/ Phthalocyanines
MX	Metal Salt
NPs	Nanoparticles

P	Phosphorescence
PDT	Photodynamic Therapy
R	Substituents
RT	Room temperature
SiNPs	Silica Nanoparticles
SubPcs	Subpthalocyanines
TCSPC	Time Correlated Single Photon Counting
TEM	Transmission Electron Microscope
TEOS	Tetraethyl Orthosilicate
Uv-Vis	Ultraviolet-Visible
XPS	X-ray Photoelectron Spectroscopy
XRD	X-ray Powder Diffraction

LIST OF SYMBOLS

α	Non-peripheral position
β	Peripheral position
ΔAS	Change in singlet state absorbance
ΔAT	Change in triplet state absorbance
ε	Molar extinction coefficient
ε_S	Singlet state molar extinction coefficient
ε_T	Triplet state molar extinction coefficient
λ	Lambda
τ_F	Fluorescence lifetime
τ_T	Triplet state lifetime
ϕ_F	Fluorescence quantum yield
ϕ_T	Triplet state quantum yield
ϕ_Δ	Singlet oxygen quantum yield
A/abs	Absorbance/absorption
E	Energy
F	Area under fluorescence emission curve
S_0	Singlet ground state
S_1	Singlet excited state
T_1	Triplet excited state
T_2	Second triplet excited state

Chapter One
Introduction

Metallophthalocyanines (MPcs) when conjugated to various nanoparticles have been researched due to their promising improved physico-chemical properties, which are of importance in many applications such as in photodynamic therapy (PDT). This work explores phthalocyanine-silica nanoparticle conjugates in the hope of improving the physico-chemical properties of phthalocyanines.

This chapter highlights the basic structure of phthalocyanines (Pcs), and subpthalocyanines (SubPcs), their application and syntheses. A basic background on silica nanoparticles (SiNPs), their syntheses and applications are also presented.

1.1 Phthalocyanines (Pcs) and Subphthalocyanine (SubPcs)

1.1.1 Brief history and general applications

Phthalocyanines were accidentally discovered by Braun and Tcherniac [**1**] and ever since then, they have been the centre of research.

Phthalocyanines are 18 π electron containing macrocyclic compounds with a 2-dimensional structure consisting of isoindole units which are connected together by nitrogen atoms [**2-4**]. Various substituents can be attached on either the periphery (β) or the non-periphery (α) positions of the macrocycle as shown in **Scheme1.1** [**5-8**]. About 70 metals and metalloids have been incorporated into the Pcs cavity [**3**]. Due to properties such as chemical and thermal stability, high molar extinction coefficients, absorption in the near-infrared [**9**], and the intense blue-green color, MPcs have been applied in many fields such as in textiles for pigmentation [**3**], photodynamic therapy (PDT) [**10**], inactivation of bacteria [**11**], sensing [**12**], nonlinear optics [**13**] and in dye sensitised solar cells [**14**]. PDT is a minimally invasive modality for the treatment of cancer. Three components are required for

PDT, i.e. a photosensitiserwhich is inactive in the dark, light of appropriate wavelength and oxygen.

SubPcs on the other hand are lower symmetry homologues of phthalocyanines. SubPcswere first discovered and documented by Meller and Ossko in 1972. They were discovered during an attempt to make a boron phthalocyanine [**15**].Their structure is composed of three isoindoline units connected together by nitrogen [**16**], an example is shown in **Scheme 1.2**. Their structure consists of 14 π electrons with boron as a central atom with an axial ligand. SubPcs have been mostly used for ring expansion in the synthesis of low symmetry phthalocyanines [**17**,**18**]. Their fused ring structure renders these class of compounds stable and they have been employed in many fields such as non linear optics [**19**], photovotaltaics, dye sensitised solar cells (DSSCs) [**20**], and electrode modification [**21**].

1.1.2 Synthesis

MPcs can be synthesized using various precursors such as phthalonitriles, phthalic anhydride, phthalic acid, phthalimide, *o*-dibromobenzene and *o*-cyanobenzamide as shown in **Scheme 1.1**. The most commonly used precursor being the phthalonitriles because they produce higher yields of MPcs and pure compounds compared to other precursors. The general synthesis is via cyclotetramerization of these precursors in the presence of a catalyst, with or without a metal salt (MX), in a higher boiling point solvent as shown in **Scheme 1.1**.

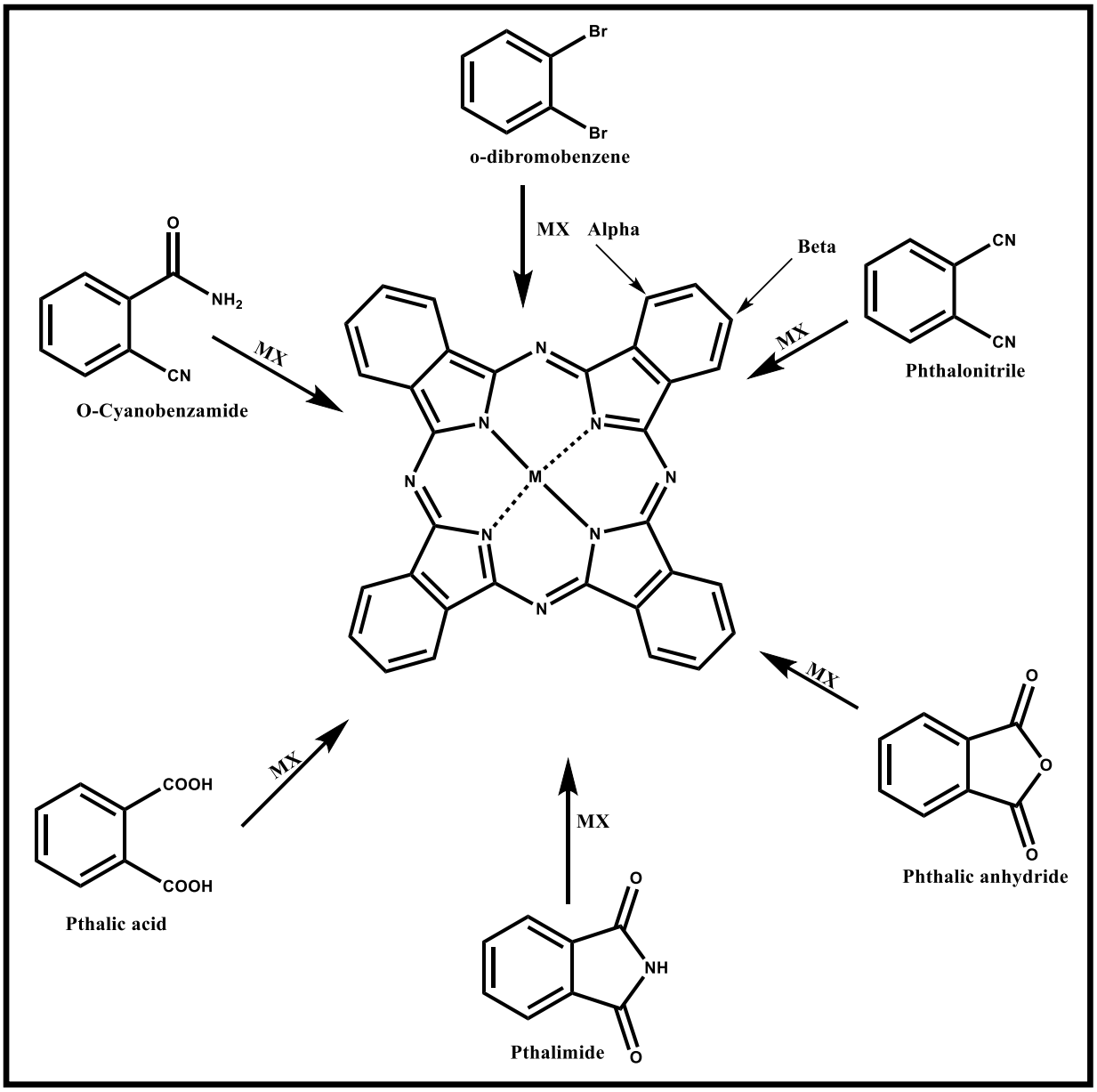

Scheme 1.1: Synthesis route of phthalocyanines (MPcs) from different precursors, MX = metal salt

Symmetrical tetrasubstituted Pcs can be synthesised by cyclotetramerization of a mono-substituted phthalonitriles in the presence or in the absence of a metal salt [**22,23**]. Low symmetry phthalocyanines can be mainly synthesised by two methods i.e. the ring expansion of SubPcs or using two differently substituted phthalonitriles

[**24**] in a static ratio of 1:3. When using the two different phthalonitriles approach, there are six possible isomers produced as shown in **Scheme 1.3** where the product of interest is separated by chromatographic techniques. Peripherally or the non-peripherally substituted MPcs may be prepared with the aid of 3 or 4-nitrophthalonitriles as shown in **Scheme 1.4**. In this thesis all the substituents were on the peripheral positions of Pcs.

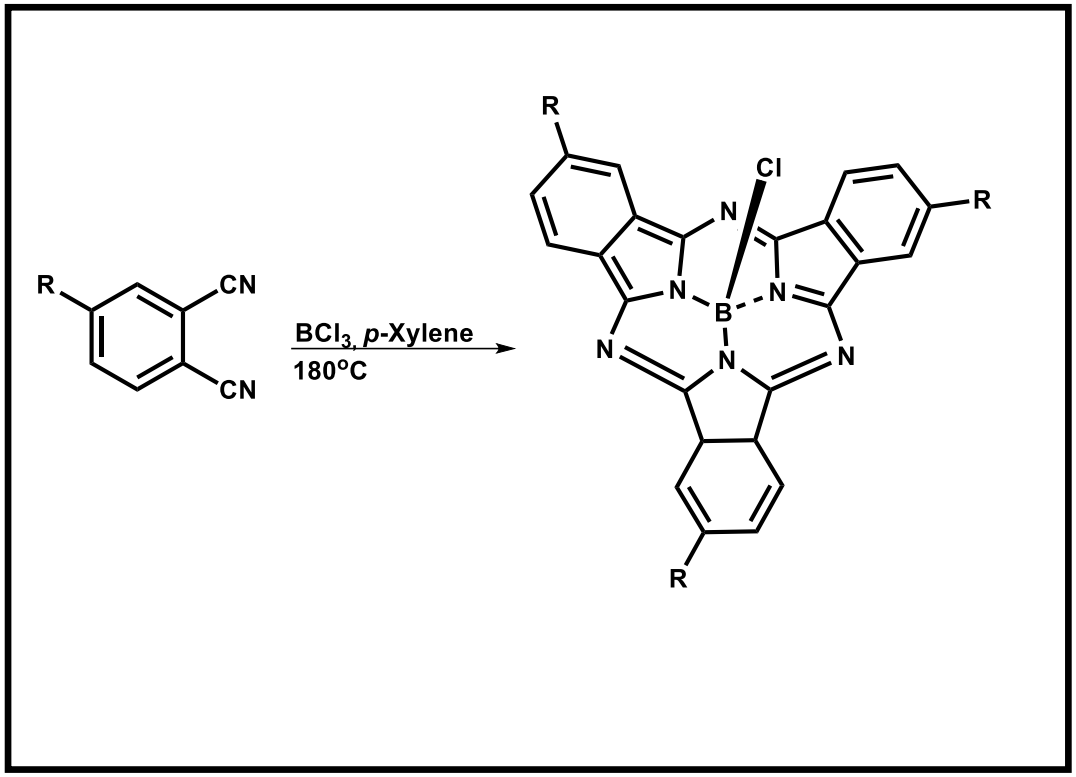

Scheme 1.2: General synthesis of SubPcs, R = Substituents.

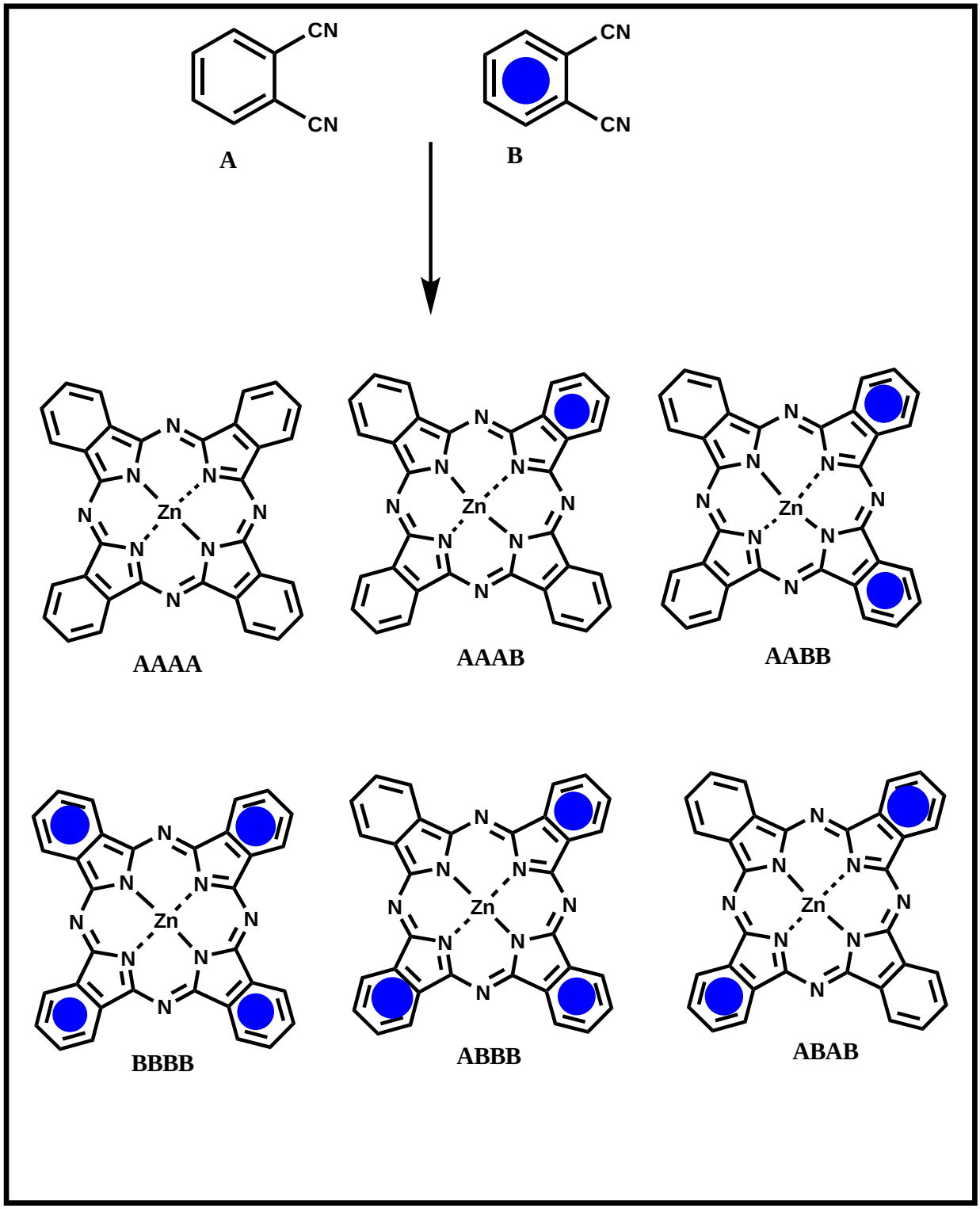

Scheme 1.3: Synthesis route of mono-substituted MPcs from phthalonitriles (**A**) and (**B**).

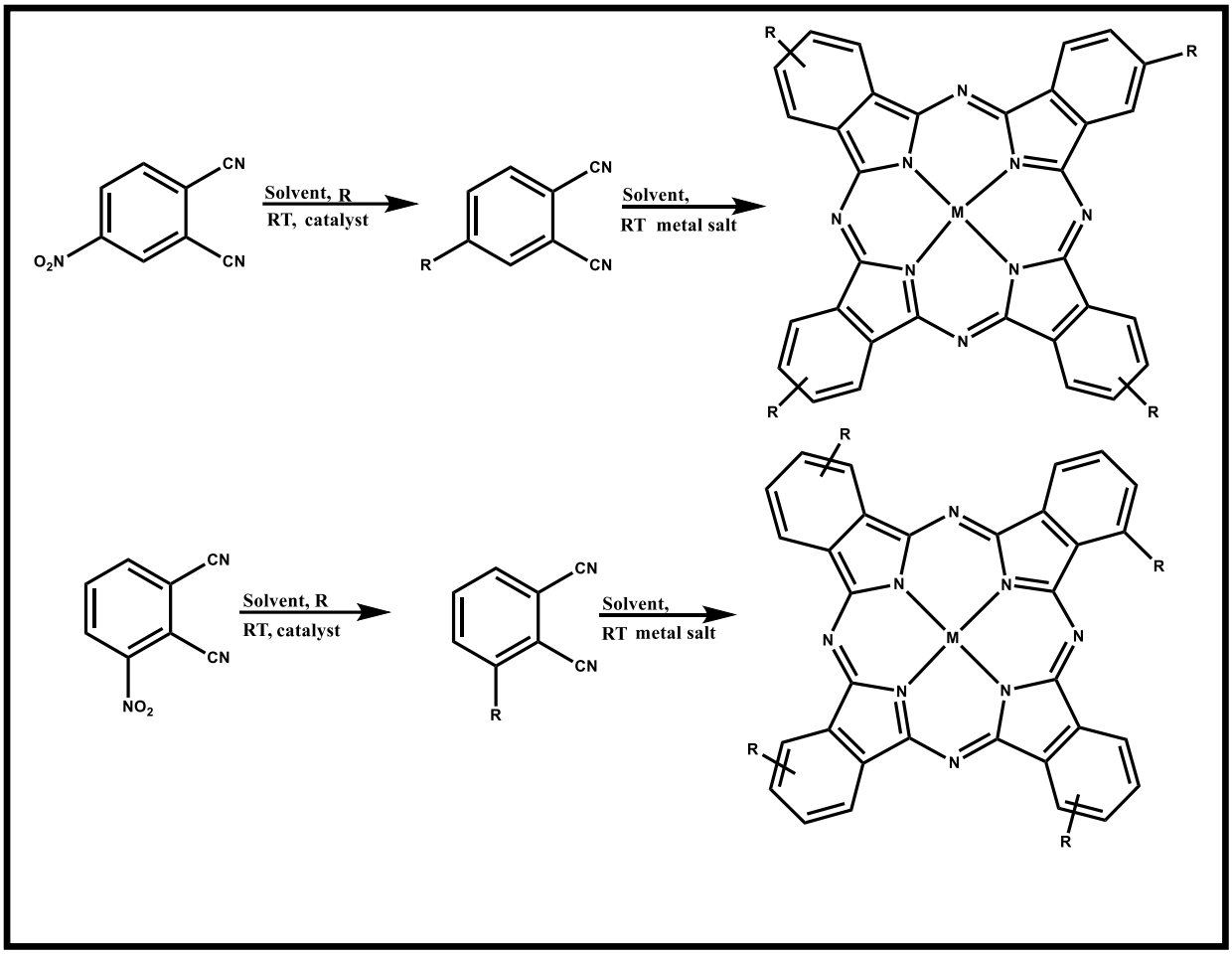

Scheme 1.4: Synthesis of (**A**) peripheral and (**B**) non-peripheral tetra-substituted MPcs from mono-substituted phthalonitriles. **RT** - Room temperature, **R** – substituents.

Synthesis of SubPcs like MPcs is through cyclization of substituted phthalonitriles in the presence of trichloroboron acid and *p*-xylene. Contrary to Pcs, trisubstituted SubPcs only have one isomer C_{2v} [**25**] as shown in **Scheme 1.2**. Synthesis of low symmetry SubPcs is difficult, however, there area few that have been reported in literature [**25**,**26**]. To improve their properties, structural modification on the periphery or substitution of the axial ligand can be done [**21**,**27**,**28**]. To shift their absorption to the near-IR, electron donating groups can be attached on the ring. In this

work,electron donating groups were both used as axial ligands and as substituents on the peripheral positions of the SubPc.

1.1.3 Electronic Absorption spectral behaviour of MPcs/ SubPcs

The spectra of phthalocyanines consist of a weak B-band and an intense Q-band as shown in **Figure 1.1(A)**. The Q and B-band transitions can be better explained by Gourteman model of linear combination of atomic orbitals (LCAO) [**29**]. The Q-band arises from transitions between the highest occupied molecular orbitals (HOMO (a_1u)) to lowest unoccupied molecular orbitals (LUMO (e_g)) of the macrocycle. B-band consists of two bands, B_1 and B_2 which arise from the transitions between a_2u and b_2u of the HOMO to e_g of the LUMO as shown in **Figure 1.2** [**30**,**31**].

The electronic absorption spectral behaviour of SubPcs is the same as that of its higher homologues MPcs, in that they resemble typical Q, and Soret (B) bands. The Q-band of these compounds is blue shifted owing to their 14 π system as shown in **Figure 1.1(B)** [**32**].

(A)

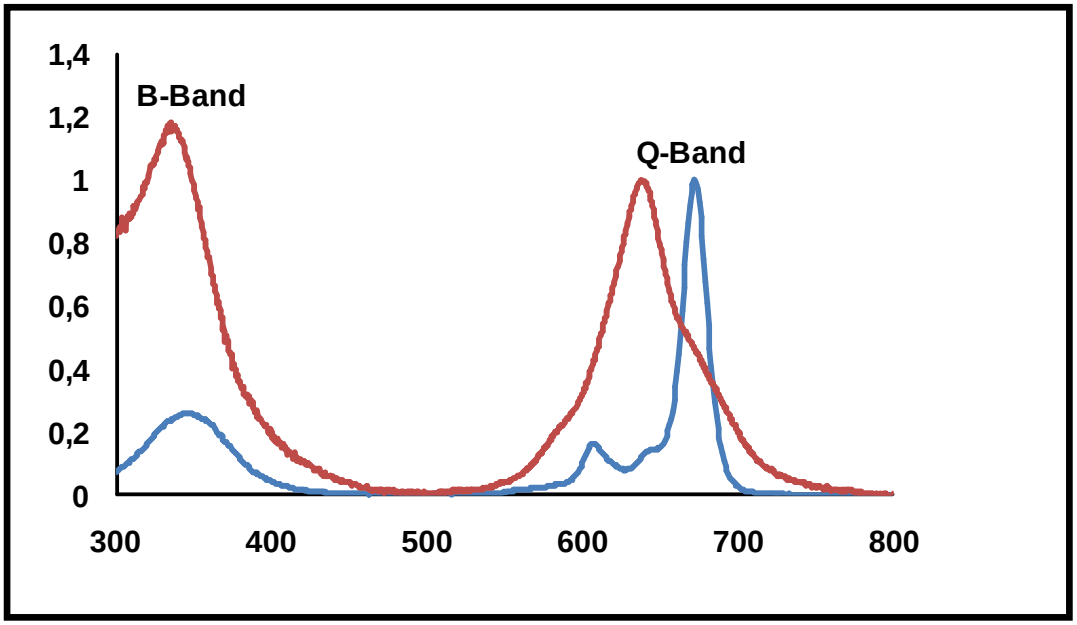

(B)

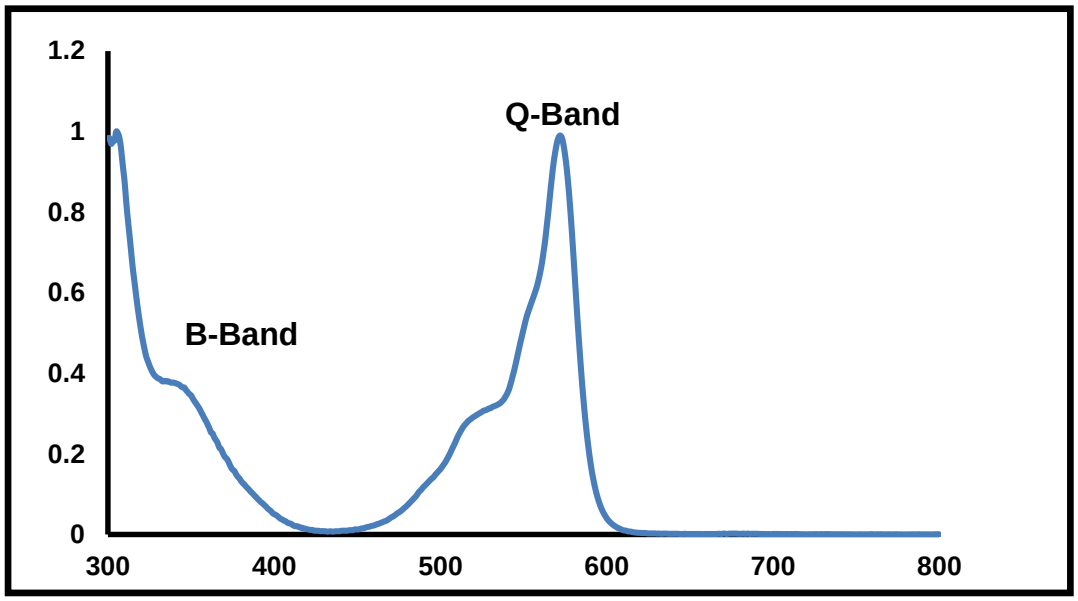

Figure 1.1: Uv-Vis spectra showing the ground state absorption spectra of a (**A**) monomeric MPc (blue) and aggregated MPc (red), (**B**) SubPc [unpublished work].

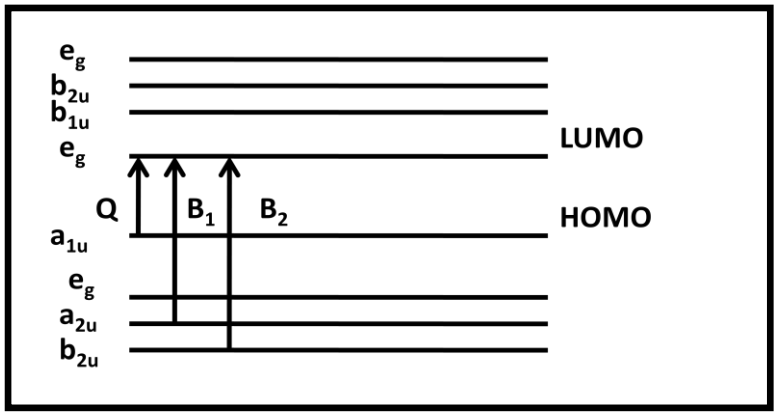

Figure 1.2: Electronic transitions in MPcs showing the origin of Q and B absorption bands.

MPcs are known to aggregate in both aqueous and some organic solvents. The Q band of phthalocyanines is narrow due to the presence of monomeric species, in the presence of aggregates the Q-band broadnes or splits due to the presence of dimers or higher oligomers as shown in **Figure 1.1(A)** [**33**,**34**]. The most common aggregates are the so called H-aggregates. Aggregation adversely affects the photophysical behaviour of MPc [**35**,**36**], since aggregates self quench singlet excited states.

1.1.4 Photophysical and Photochemical properties of Pcs and SubPcs.

Photophysico-chemical properties of MPcs and SubPcs are best described using the Jablonski diagram. **Figure 1.3** gives a detailed picture of the processes that are occurring at the electronic level. MPcs and SubPcs can absorb light in their ground state (**S_0**) to the first excited state (**S_1**) where they can undergo intersystem crossing to the first triplet excited state or undergo fluorescence in the process. In their triplet excited state, they may transfer their energy to molecular oxygen (**$^3O_2$**), generating a

reactive singlet oxygen species ($^1O_2$) or undergo phosphorescence. Singlet oxygen species is the main component involved in PDT, photodegradation etc, and is of interest in this work.

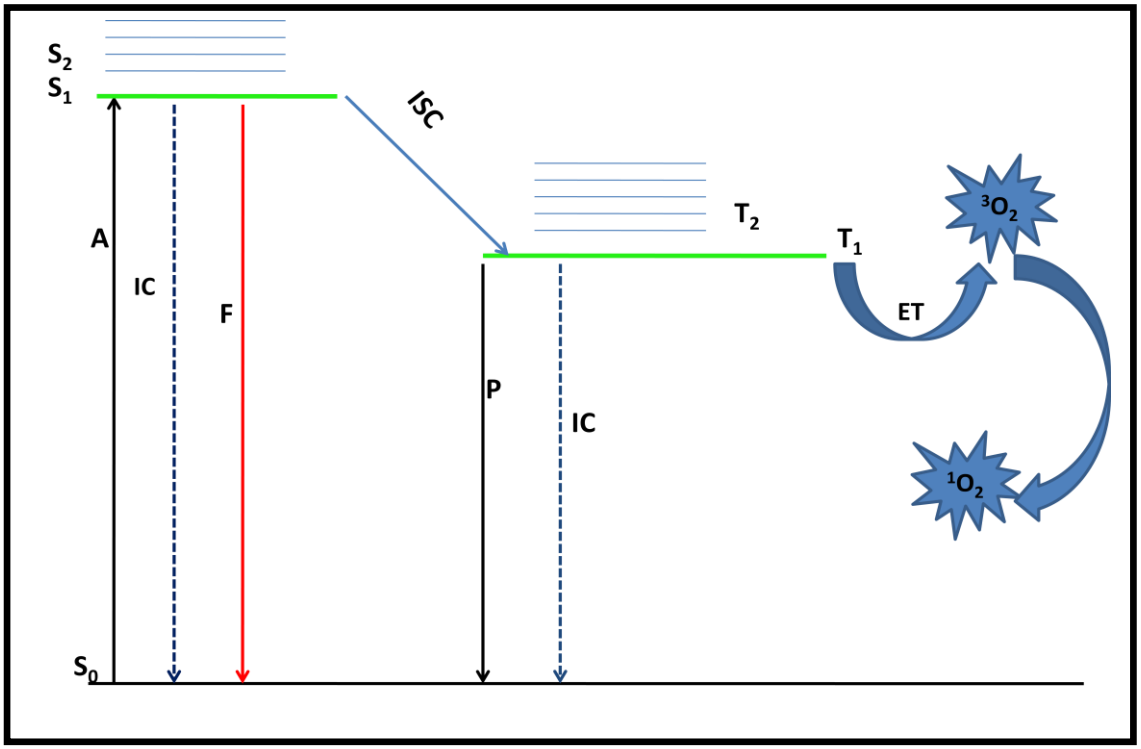

Figure 1.3: A modified Jablonski diagram: **A**=Absorbance, **S_0**=Ground state, **S_1**= First excited state, **S_2**=Second excited state, **IC**=Internal conversion, **F**=Fluorescence, **ISC**=Intersystem crossing, **P**=Phosphorescence, **ET**=Energy transfer, **T_1**=First triplet state, **T_2**=Second triplet state, **$^3O_2$**= Oxygen in its triplet state, **$^1O_2$**=Singlet oxygen.

1.4.1.1 Fluorescence quantum yields (ϕ_F) and lifetimes(τ_F)

Fluorescence quantum yield is the ratio of absorbed photons to the emitted photons through fluorescence. Fluorescence quantum yields can be determined by comparative or absolute methods [**37**]. The comparative method uses fluorescence quantum yields of a standard as a reference and was used in this work. The fluorescence quantum yields can be determined using equ. (1.1)

$$\phi_F = \phi_F^{Std} \frac{FA^{Std}n^2}{F_{Std}An_{Std}^2} \quad \textbf{(1.1)}$$

where***F*** and F_{STD} are areas under fluorescence emission curves of the sample and the standard, respectively. ***A*** and A_{STD} are the absorbances of the sample and standard at the excitation wavelength, respectively, **n** and n_{STD} are refractive indices of solvents used for sample and standard, respectively. ZnPc in dimethyl sulfoxide (DMSO) was used as a standard, ϕ_F= 0.20 [**38**], in this work for MPcs and Rose Bengal in ethanol was used as a standard for SubPcs, ϕ_F= 0.11 [**39**]. For the determination of fluorescence quantum yields, the sample and the standard are both excited at the same wavelength.

Fluorescence lifetimes are defined as the time a fluorophore spends in the excited state before it relaxes back to the ground state through fluorescence. Time–correlated single photon counting technique (TCSPC) was used to determine the fluorescence lifetime (a typical fluorescence decay curve is shown in **Figure 1.4** [**40**].

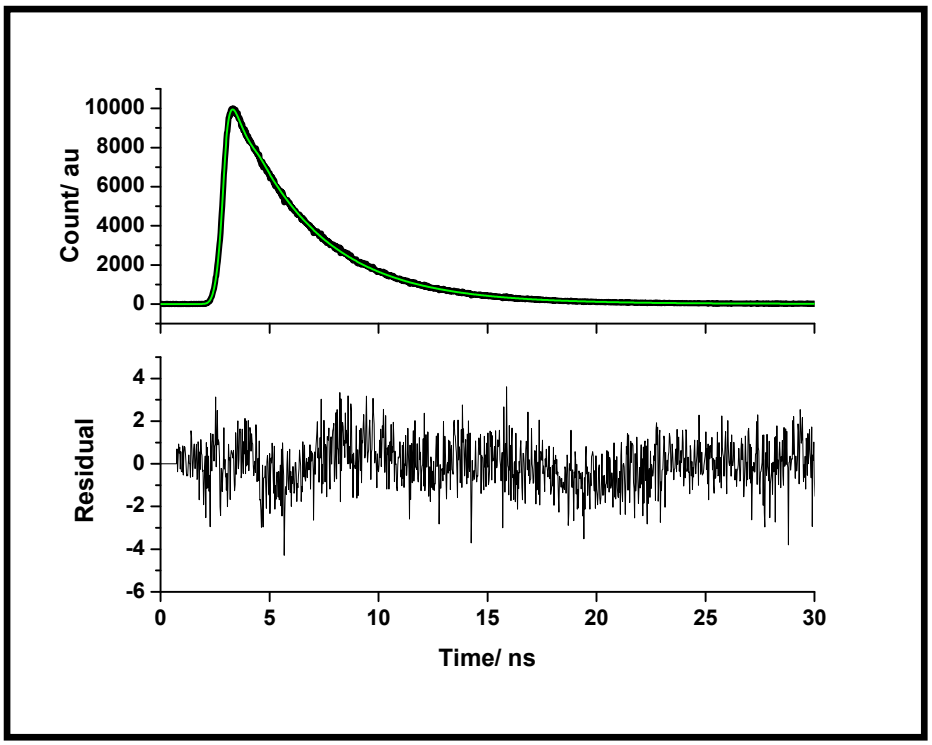

Figure 1.4: Fluorescence decay curve in DMSO [**40**]

1.4.1.2 Triplet quantum yields ϕ_T and lifetimes τ_T

The triplet quantum yield (ϕ_T) is used to estimate the efficiency of the molecule to populate the triplet state.There are various methods of studying the properties of a molecule in its triplet state [**41**–**43**]. The laser flash photolysis technique was used in this thesis through comparative methods where ZnPc was used as a standard and calculations were done using equ. (1.2)

$$\phi_T = \phi_T^{STD} \frac{\Delta A_T . \varepsilon_T^{STD}}{\Delta A_T^{STD} . \varepsilon_T} \quad \textbf{(1.2)}$$

where ΔA_T and ΔA_T^{STD} are the changes in the triplet state absorbances of the sample and the standard respectively. ε_T and ε_T^{STD} are the triplet state molar extinction coeffients for the sample and the standard respectively. ϕ_T^{STD} is the triplet state

quantum yield for the unsubstituted ZnPc standard $\boldsymbol{\phi_T^{STD}}$= 0.65 in DMSO [**44**]. $\boldsymbol{\varepsilon_T}$ and $\boldsymbol{\varepsilon_T^{STD}}$ were calculated from the molar extinction coefficients of their respective ground singlet state ($\boldsymbol{\varepsilon_S}$), the changes in absorbances of the ground state($\Delta \boldsymbol{A_S}$) or the triplet state ($\Delta \boldsymbol{A_T}$**)** using equ. (1.3 a) and (1.3 b).

$$\boldsymbol{\varepsilon_T = \varepsilon_S . \frac{\Delta A_T}{\Delta A_S}} \quad \textbf{(1.3 a)}$$

$$\boldsymbol{\varepsilon_T^{STD} = \varepsilon_S^{STD} . \frac{\Delta A_T^{STD}}{\Delta A_S^{STD}}} \quad \textbf{(1.3 b)}$$

Triplet lifetimes are then determined by fitting data into Origin 8, a typical fitted decay curve is shown in **Figure 1.5**[**45**].

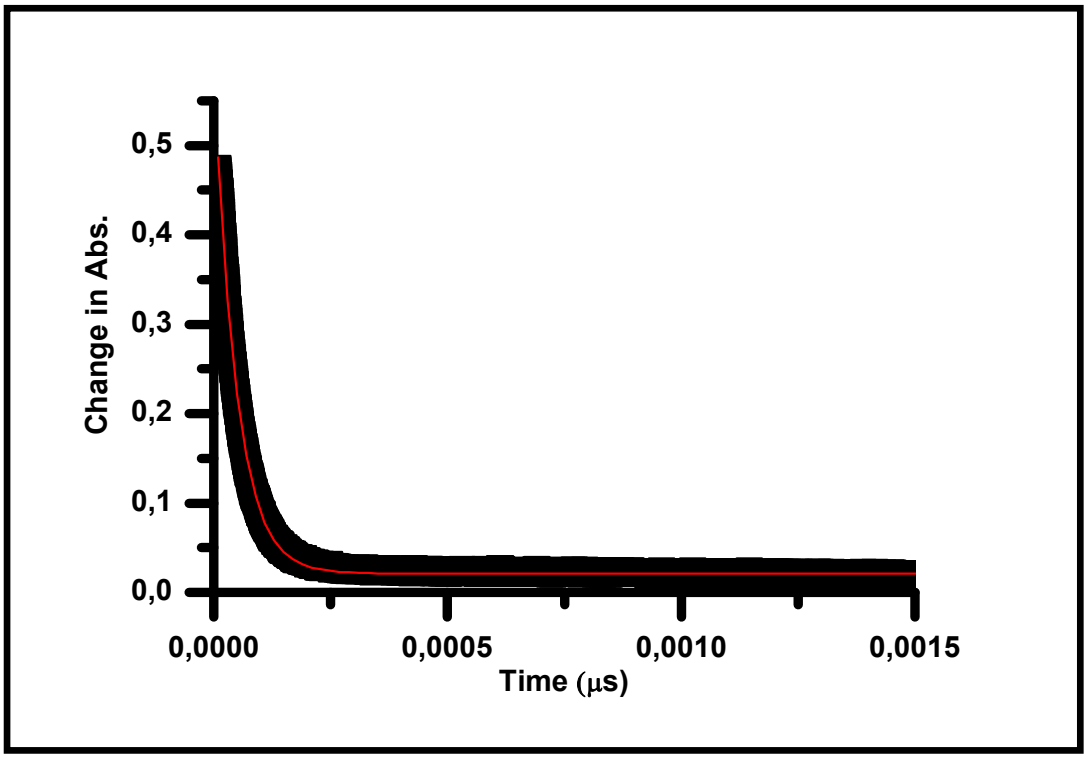

Figure 1.5: Typical decay curve in DMSO [**45**].

1.1.4.3 Singlet oxygen quantum yield (ϕ_Δ)

Singlet oxygen quantum yield ($\boldsymbol{\phi}_\Delta$) can be defined as the amount of $^1O_2$ generated per photon absorbed by the phthalocyanine/subpthalocyanine complex. Singlet oxygen species can be quantified experimentally by two methods, i.e. singlet oxygen luminescent and chemical methods. The chemical method was used in this work, and it requires a singlet oxygen quencher that will react with singlet oxygen as soon as it is produced in an oxygenated solution. Spectroscopic methods are then used to monitor production of singlet oxygen through the decay profile of a scavenger [**46**].

In this work 1,3-diphenylisobenzofuran (DPBF) in organic solvents, and anthracene-9,10-bis-methylmalonate (ADMA) in water were used as singlet oxygen scavengers. Equ. (1.4) was then used to calculate singlet oxygen quantum yields:

$$\boldsymbol{\phi}_\Delta = \boldsymbol{\phi}_\Delta^{STD} \frac{\boldsymbol{R}^{Sample}.\boldsymbol{I}_{Abs}^{STD}}{\boldsymbol{R}^{STD}.\boldsymbol{I}_{Abs}^{Sample}} \qquad \textbf{(1.4)}$$

Where $\boldsymbol{\phi}_\Delta^{STD}$ is the singlet oxygen quantum yield for the standard (ZnPc, $\boldsymbol{\phi}_\Delta^{STD}$ = 0.67 in DMSO [**47**]) and $\boldsymbol{\phi}_\Delta^{STD} = 0.58$ in toluene [**38**]. AlPcSmix (containing a mixture of sulfonated phthalocyanine derivatives) was employed as a standard in aqueous media ($\boldsymbol{\phi}_\Delta^{STD}$ = 0.42) [**47**]. Rose Bengal was employed as a standard for SubPcs in ethanol ($\boldsymbol{\phi}_\Delta^{STD}$ = 0.68) [**48**]. $\boldsymbol{R}^{Sample}$and $\boldsymbol{R}^{STD}$are the DPBF and ADMA photobleaching rates in the presence of the sample under investigation and the standard, respectively**.** $\boldsymbol{I}_{Abs}^{Sample}$and $\boldsymbol{I}_{Abs}^{STD}$ are the rates of light absorption by the sample and the standard, respectively and are calculated using equ. (1.5a) and (1.5b)

$$\boldsymbol{I}_{Abs}^{Sample} = \frac{\alpha.A.I}{N_A} \qquad \textbf{(1.5a)}$$

$$I_{Abs}^{STD} = \frac{\alpha.A.I}{N_A} \quad \textbf{(1.5b)}$$

where $\alpha = 1 - 10^{-A(\lambda)}$, A (λ) is the absorbance of the sensitizer at the irradiation wavelength, A is the irradiated area, I is the intensity of light expressed as photons (cm^{-2} s^{-1}) and N_A is Avogadro's constant.

1.1.5 MPcs and SubPcs used in this thesis

Pcs and SubPcs used in this work are shown in **Table 1.1**. Complexes **1-5** [**5**,**49**-**51**] are known, while **6, 7** and **8** are new. The photophysical properties of complex **5** are however reported for the first time in this thesis. All the MPcs that are reported in this work contain Zn as a central metal. This is because Zn containing MPcs are known to have high triplet quantum yields with corresponding high singlet quantum yields and they also have longer triplet lifetimes [**36**,**52**]. MPcs carrying charges are often soluble in aqueous media which is of importance in applications like PDT. Herein this thesis reports on the efficiency of charged MPcs towards the generation of singlet oxygen when doped onto SiNPs i.e. positively charged (**3**) versus negatively (**4**) charged, and neutral (**1**) and (**2**).

A low symmetry MPc (**6**) was both conjugated and doped to SiNPs and the effect of doping versus conjugation was investigated. Asymmetrical Pcs are known to improve triplet state population [**53**], hence complex **6** is employed and the effect of doping versus linking to SiNPs on the triplet state parameters and singlet oxygen generation were assessed. Mercaptopyridine were employed for **6**as substituents in order to improve solubility due to its bulky nature. Thiazoles are known photosensitisers [**54**] and their linking to MPcs may improve PDT parameters, since they are both photosensitisers [**55**–**57**], hence a thiazole is employed for **6**.

Complex **5** was obtained with the aim of doping onto SiNPs, but for reasons explained in the discussion, this did not work but its synthesis and photophysical properties are reported.

Synthesis of SubPcs (**7** and **8**) was also attempted and their photophysical properties were determined.

Table 1.1: showing MPcs employed in this work.

Complex	**Complex number**	**Bond formed**	**Ref.**
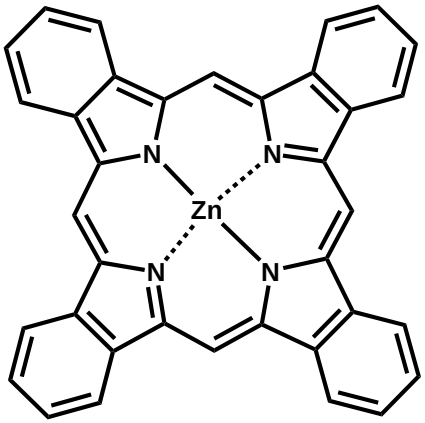 **Unsubstituted ZnPc**	**(1)**	Doped	Available commercially

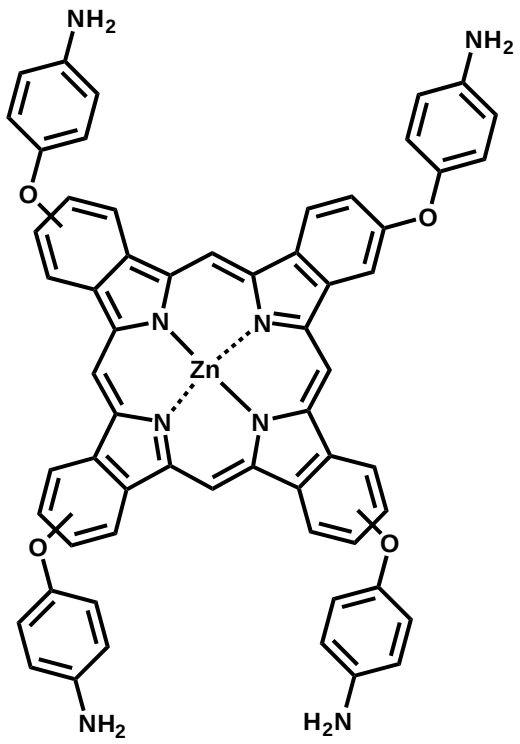 **Zn tetraaminophenoxyphthalocyanine**	**(2)**	Doped	[**49**]
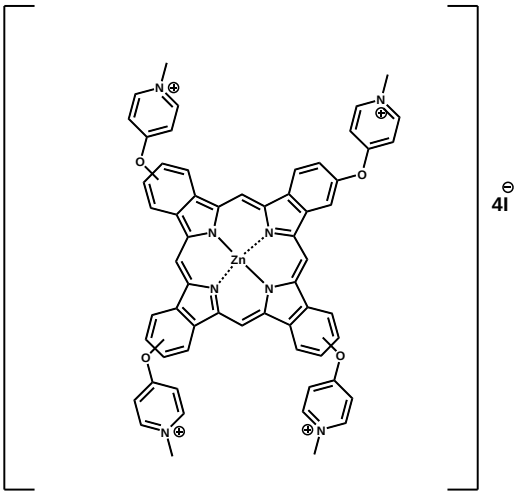 **Zntetrakis[4-(iodo-N-methylpyridinium)thio]phthalocyanine**	**(3)**	Doped	[**5**]

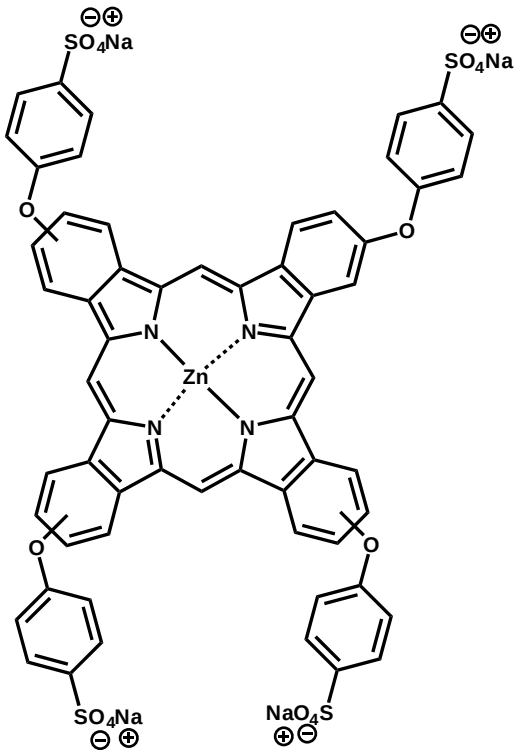 **Zntetrasulfophenoxyphthalocyanine**	**(4)**	Doped	[**50**]

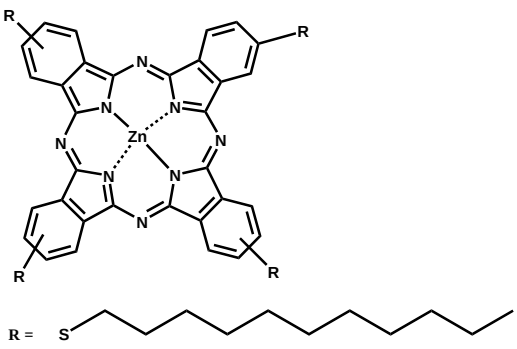 **Zn tetra-kis-(dodecylmercapto) phthalocyanine**	**(5)**	-	[**51**]
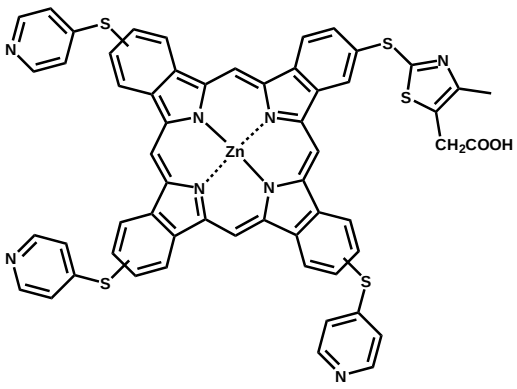 **Zn tris[(4-(pyridin-4-ylthio)2- thio-4-methylthiazol-5yl)acetic acid phthalocyanine**	**(6)**	Linked and doped	New

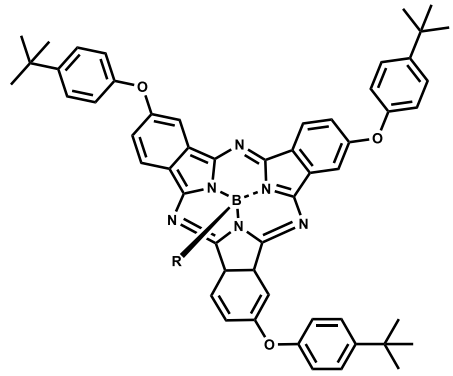 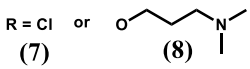 R = Cl or (7) (8) **Chloro (2,9,16(2,9,17))tris-(tert-butylphenoxy) subphthalocyanine boron (II) (7)** **Or** **N,N-dimethyl-3-(l1oxidanyl)propan-1-amine (2,9,16(2,9,17))-tris-(tertbutylphenoxy) subphthalocyanine boron (II) (8)**	**(7)** or **(8)**	-	New

1.2 Silica nanoparticles

1.2.1 Background and Applications

Nanoparticles (NPs) are materials with sizes that range from 1-100 nm in diameter. These materials have unique properties that are different from their bulk counter parts [**58**]. Their unique properties are controlled by their sizes, composition, crystalline behaviour and shape. A number of NPs have been subjected to research due to their unique properties; these include quantum dots [**12**], silver [**59**], gold [**9**,**59**] and silica NPs amongst others. SiNPs are employed in this work hence are discussed in detail.

This work focused on SiNPs due to properties which include: ease of functionalization, high surface area, biocompatibility, chemical inertness [**60**]. Because of these interesting properties, SiNPs have been applied in various fields such as bio-imaging [**61**], gene therapy, as drug delivery agents for cancer treatment [**62**], biomarkers, biosensors [**61**] amongst other applications.

1.2.2 Syntheses

SiNPs can be synthesized via two methods i.e. the Stober method and reverse micro-emulsion. The Stober method requires the use of an organo-silicate precursor (usually tetraethyl orthosilicate, TEOS), which undergoes hydrolysis in a mixture of water, ethanol and ammonia solution (acting as the catalyst) to produce silicic acid. The silicic acid then undergoes condensation to produce di-silicic acid which also goes through condensation to form amorphous silica nanoparticles, **Scheme 1.5** [**63**].

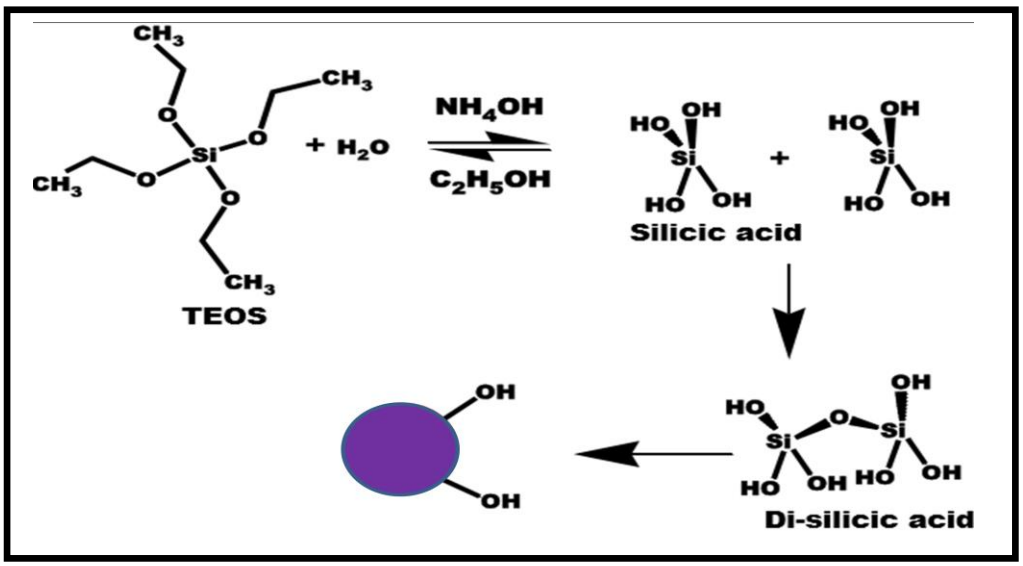

Scheme 1.5: Representation of a typical synthesis of SiNPs via the Stober protocol [**63**].

The Stober method produces uniformly shaped and sized silica nanoparticles [**63**], however, this method produces large sized nanoparticles. A number of studies have have concentrated on improving the size of SiNPs using the Stober method and have also revealed that a number of parameters such as the rate at which TEOS is added, addition of H_2O/ammonia amongst others, play a significant role in the overall size [**64**,**65**].

The reverse micro-emulsion method utilizes the hydrolysis of TEOS in a reverse micelle or water in oil micro-emulsion system, containing a homogenous mixture of water, oil surfactant and ammonium hydroxide as a catalyst. In this method, the water droplets are stabilized by the surfactant molecules thus allowing for diffusion in oil to occur. Since water droplets control the nucleation and growth process, the resulting particles are highly monodispersed, uniform, spherical and are smaller in thanthe one synthesized by Stober method. The amounts of both water and surfactant affect the size of silica particles synthesized in the micro-emulsion method [**58**,**65**,**66**]. This method has been used to encapsulate materials ranging from dyes such as Pc, as in **Figure 1.6(A)** to other nanoparticles [**58**,**67**]. The reverse micro-emulsion method was employed in this work.

Due to the dangling hydroxyl group, SiNPscan be functionalized easily. A number of groups have been attached on the surface of SiNPs with the aim of conjugating them to various compounds such as biomolecules, other NPs, and photosensitisers amongst others [**68**–**70**]. In this work SiNPs, were functionalized with amino moiety as shown in **Figure 1.6(B)**, with the aim of conjugating to a carboxylic functionalized MPc via amide bond.

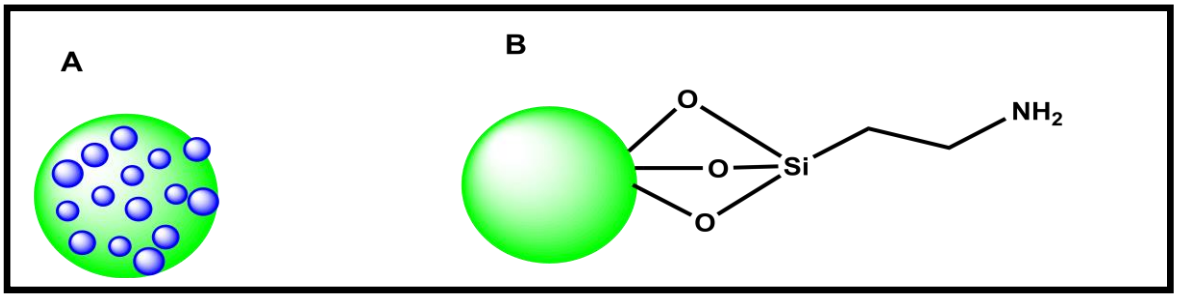

Figure 1.6: Represents (**A**) SiNPs doped with MPc (blue spheres representing MPcs) and (**B**) representing amine functionalised SiNPs

1.2.3 MPcs doped/conjugated to SiNPs and their applications

A number of MPcshave been conjugated to SiNPs either via physical or chemical methods. Improvement in the photophysico-chemical properties of MPcshave been observed following conjugation/doping. **Table 1.2** lists some of the MPcs that have been conjugated/doped to SiNPs and applications in literature [**68**, **71**-**75**].**Table 1.2** shows that mainly symmetrical Pcs have been employed for doping into SiNPs with only a few examples of asymmetrical Pcs. The asymmetric Pcs employed in literature do not have bulky substituents (which are employed in this thesis for **6**), bulky substituents improve solubility. This thesis is the first to report asymmetrical Pc with bulky functional groups linked to SiNPs. Asymmetry improves triplet state parameters. Charged MPcs have been doped onto SiNPs [**50**], however their photophysics are reported here for the first time.

Table 1.2: Shows some of the MPcs conjugated to SiNPs and their applications

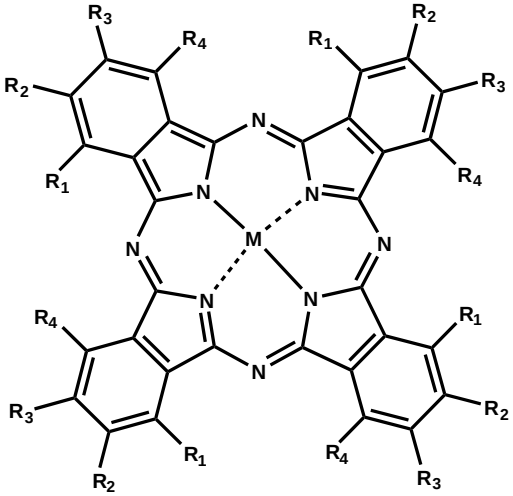

Complex	Application	Bond	Ref.
M = Co **$R_1 = R_2 = R_4 = H$** **R_3 =** 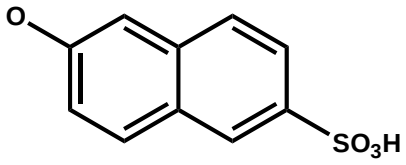	Catalyst in oxidation of thiols	Doped	[**71**]
M = Co **$R_1 = R_2 = R_4 = H$** **R_3 =** 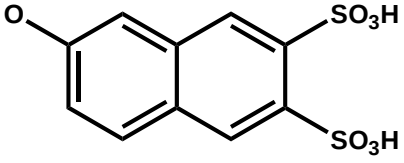	Catalyst in oxidation of thiols	Doped	[**71**]

M = Zn **$R_1 = R_2 = R_4 = H$** **$R_3 =$** 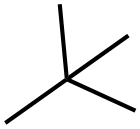	PDT	Doped	[**72**]
M = Zn or AlCl **$R_1 = R_2 = R_4 = H$** **$R_3 =$** 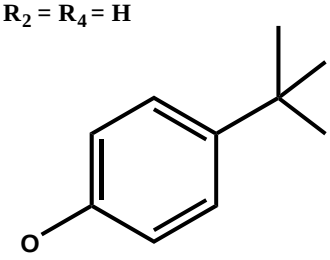	-	Doped	[**68**]
M = Zn **$R_1 = R_2 = R_3 = H$** **$R_4 =$** 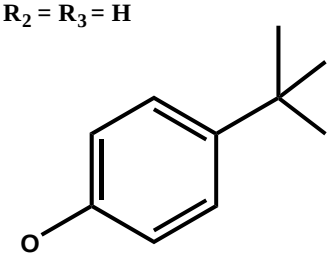	-	Doped	[**68**]
M = Zn **$R_1 = R_2 = R_4 =$ H** **$R_3 =$** 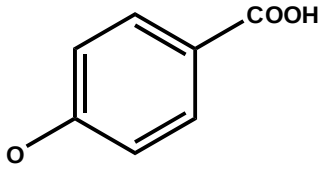	-	Doped	[**68**]
	Artificial lysosomal fluid	Amide	[**73**]
	-	Doped	[**74**]

M = Zn **$R_1 = R_2 = R_3 = H$** **R_4 =** 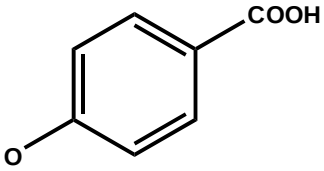	-	Doped	[**74**]
M = Zn **$R_1 = R_2 = R_3 = H$** **R_4 =** 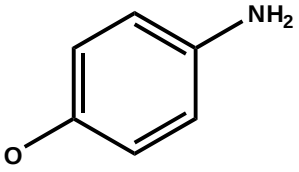	-	Amide	[**75**]
M = Zn **$R_1 = R_2 = R_4$ =** **H** **R_3 =** 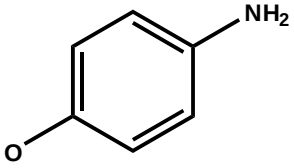		Amide	[**75**]
M = Zn **$R_1 = R_2 = R_3 = H$** **R_4 =** **NH_2**		Amide	[**75**]

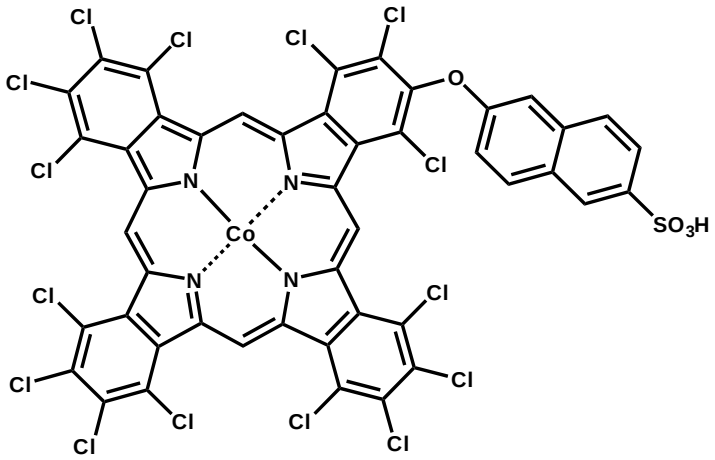	Catalyst in oxidation of thiols	Doped	[**71**]

1.3 Aims.

1. Synthesis and characterization of symmetrical MPcs bearing differently charged or neutral substituents.
2. Synthesis and characterization of amino functionalized SiNPs
3. Synthesis and characterization of low symmetry phthalocyanine with a carboxylic terminal group.
4. Doping MPcs onto SiNPs.
5. Evaluating the photophysical properties; comparing the influence of charge before and after doping
6. Linking of asymmetrical Pc to SiNPs via an amide bond
7. Evaluating the enhancement of singlet oxygen (conjugation vs doping)
8. Synthesis and characterization of SubPc.
9. Evaluation of photophysical properties of SubPc.

Chapter Two
Experimental

2.1 Material

2.1.1 Solvents

Ultra-pure water was obtained from a milli-pore water system. Dimethyl sulfoxide (DMSO), dimethylformamide (DMF), cyclohexane, ammonia, hexanol, n-pentanol, methanol, ethanol, ethyl acetate, isopropanol, toluene, *p*-xylene, hexane and pyridinewere purchased from Minema.Trichloroboron (BCl_3), 3-dimethylamino-1-propanolwere purchased from Merck. Triton X-100, and deuterated dimethylsulfoxide (DMSO-d_6) were purchased from Sigma Aldrich.

2.1.2 Previously synthesized phthalonitriles and MPcs

Unsubstituted zinc phthalocyanines (complex **1**) and zinc acetate $(ZnOAc)_2$ were purchased from Sigma Aldrich. 1,8-Diazabicyclo[5.4.0]undec-7-ene (DBU) was purchased from Merck. 4-Pyridylthiophthalonitrile (**6a**) [**5**], 4,5-(2-mercapto-4-methyl-5-thiazoleaceticacid) phthalonitrile (**6b**) [**76**], **Scheme 3.2** and 4-(4-tert-butylphenoxy) phthalonitrile (**7a**) [**77**] were synthesized according to literature. zinc tetra (4-aminophenoxy) phthalocyanine(complex **2**) [**49**], zinc tetrakis[4-(iodo-N-methylpyridinium)oxy] phthalocyanine(complex **3**) [**5**], zinc tetra(4-sulfophenoxy) phthalocyanine (complex **4**) [**50**], and zinc tetrakis (dodecylmercapto) phthalocyanine (complex **5**) [**51**] were synthesized and purified as reported in literature.

2.1.3 Other reagents

Tetraethyl orthosilicate (TEOS), 1,3-diphenylisobenzofuran (DPBF),anthracene-9,10-bis-methylmalonate (ADMA), 3-aminopropyl)triethoxysilane(APTES), 2-mercapto-4-methyl-5-thiazoleacetic acid, *N,N'*-dicyclohexylcarbodiimide (DCC) and 4-dimethylaminopyridine (DMAP) were purchased from Sigma Aldrich, AlPcSmix

(containing a mixture of sulfonated phthalocyaninederivatives) was prepared as reported in literature [**78**].

2.2. Equipment

i. ^{1}H nuclear magnetic resonance signals were recorded on a Bruker AMX 400 MHz NMR spectrometer.

ii. Elemental analyses for CHNS were done using a Vario-ElementarMicrocube ELIII Series.

iii. Ground state electronic absorption spectra were performed on a Shimadzu UV-2550.

iv. Fluorescence excitation and emission spectra were recorded on a Varian Eclipse fluorescence spectrofluorimeter.

v. Fluorescence lifetimes were measured using a time correlated single photon counting setup (TCSPC) (FluoTime 200, Picoquant GmbH) with a diode laser (LDH-P-670 with PDL 800-B, Picoquant GmbH, 670 nm, 20 MHz repetition rate, 44 ps pulse width), **Figure 2.1**.

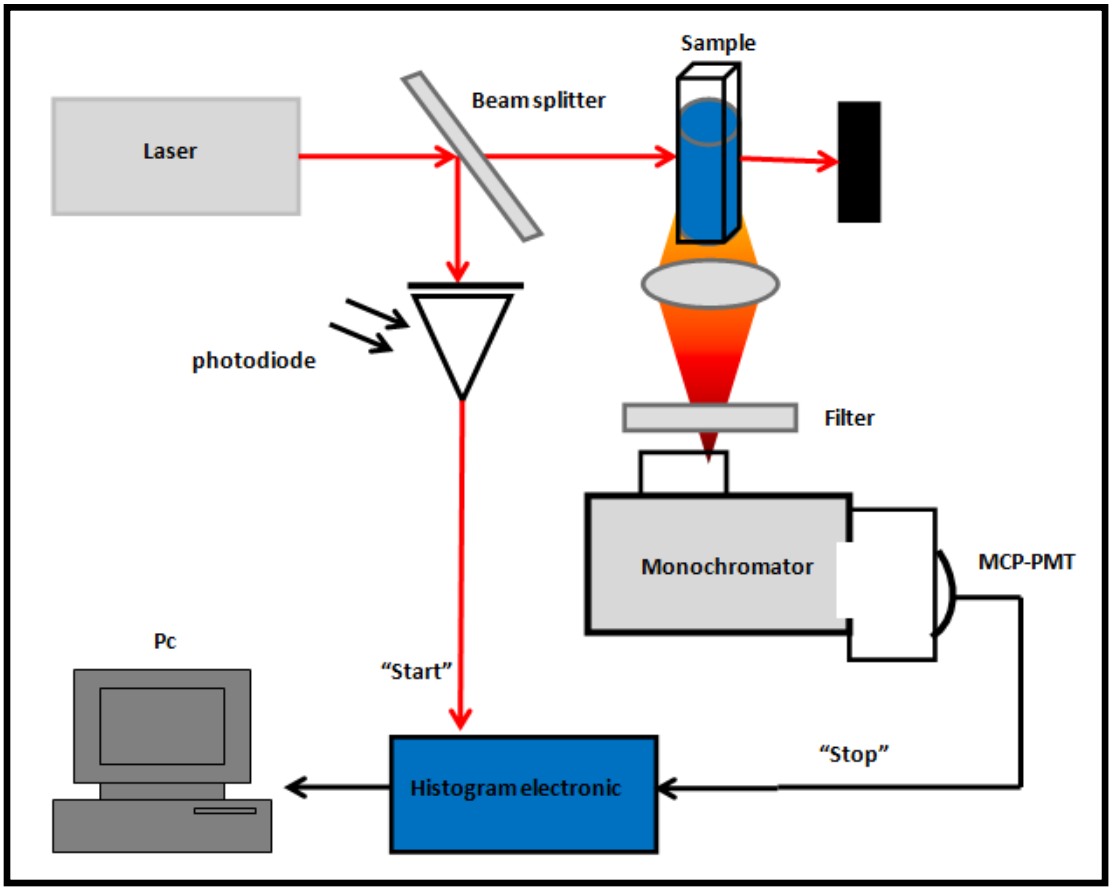

Figure 2.1: Time correlated single photon counting (TCSPC) setup

vi. Infra-red spectra were measured on Bruker® ALPHA FT-IR spectrometer.

vii. Triplet quantum yields were determined using a laser flash photolysis system. The excitation pulses were produced using a tunable laser system consisting of an Nd:YAG laser (355 nm, 135 mJ/4–6 ns) pumping an optical parametric oscillator (OPO, 30 mJ/3–5 ns) with a wavelength range of 420–2300 nm (NT-342B, Ekspla) as shown in **Figure 2.2**.

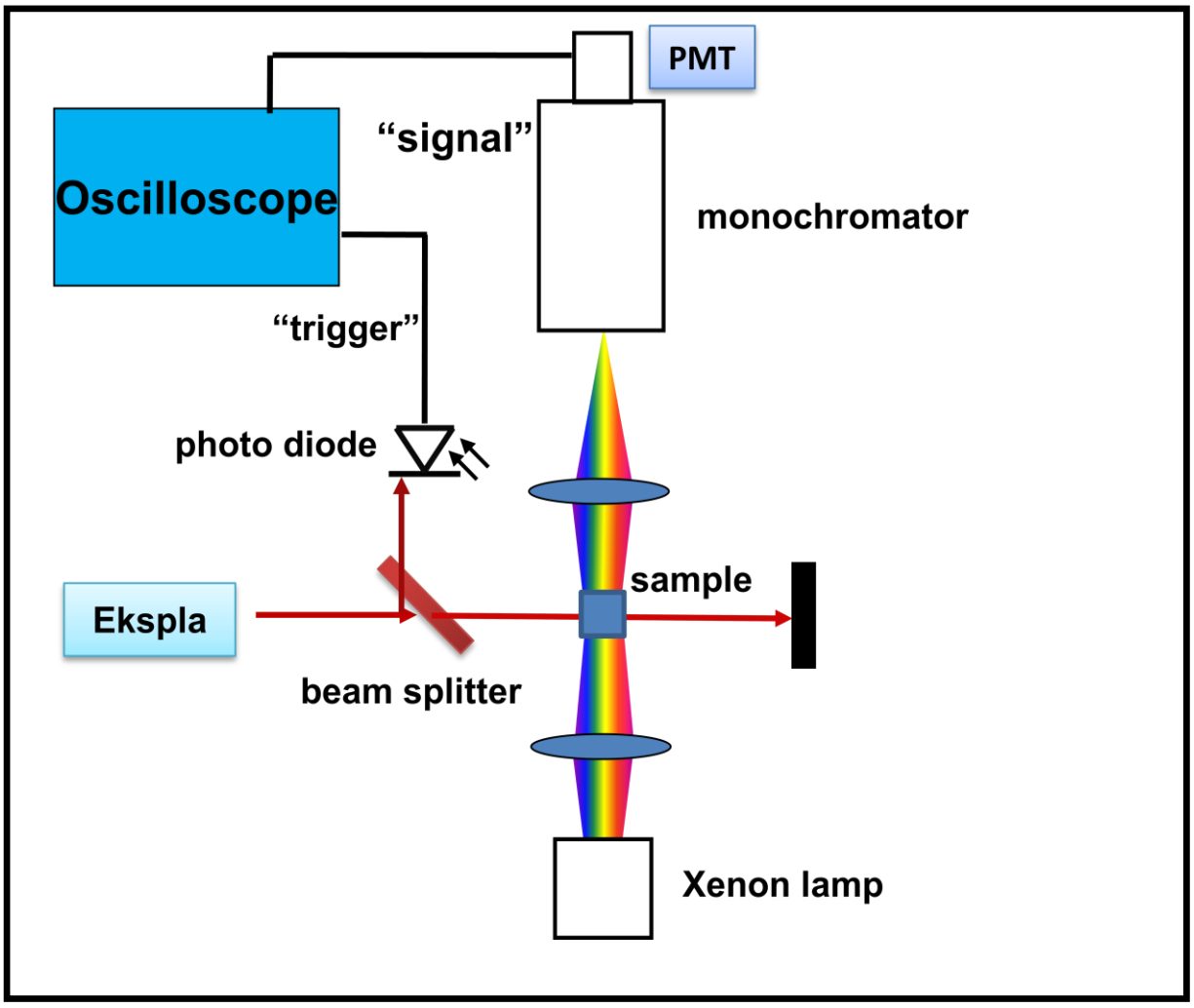

Figure 2.2: Laser flash photolysis system

viii. Singlet oxygen quantum yields were determined using a general electric quartz lamp (300W) while 600 nm glass cut off filter (Schott®) and water filter were employed to filter off ultra-violet and infrared radiation. An interference filter, 700 nm with a band of 40 nm, was placed just before the sample chamber, as shown in **Figure 2.3**. Light intensities were measured with a POWER MAX® 5100 (Molectron detector incorporated) power and were found to be 4.3×10^{15} photons $cm^{-2}s^{-1}$.

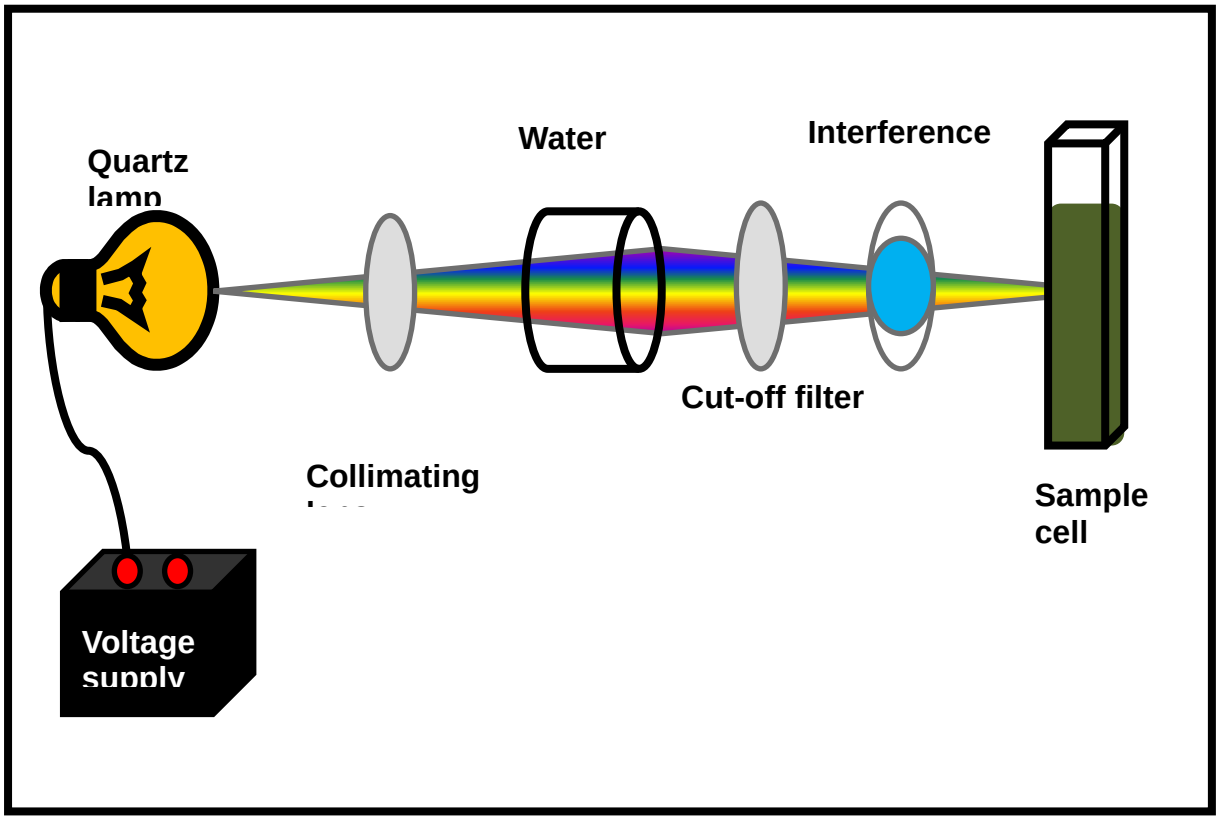

Figure 2.3: Singlet oxygen setup

ix. Transmission electron microscope (TEM) images were obtained using a JEOL TEM 1210 transmission electron microscope at 100 kV accelerating voltage. TEM samples were prepared by placing a drop of conjugates or nanoparticle solution on the sample grid and allowing it to dry before measurements.

x. X-ray powder diffraction (XRD) patterns were recorded on a Bruker D8, Discover equipped with a Lynx Eye Detector, using Cu Kα radiation (λ = 1.5405 Å, nickel filter). Data were collected in the range from 2θ = 5° to 100°, scanning at 1° min^{-1} with a filter time-constant of 2.5s per step and a slit width of 6.0 mm. Samples were placed on a zero background silicon wafer slide. The X-ray diffraction data were treated using Eva (evaluation curve fitting) software. Baseline correction was performed on each diffraction pattern by

subtracting a spline fitted to the curved background and the full width at half maximum values used in this study was obtained from the fitted curves.

xi. X-ray photoelectron spectroscopy (XPS) data were collected using a Kratos Axis Ultra DLD, using an Al (monochromatic) anode, equipped with charge neutralizer and the operating pressure kept below 5 x 10^{-9} torr. For wide/survey XPS scans, the following parameters were used: emission current was kept at 5 mA and a dual anode (Al) voltage at 15 kV. The resolution used to acquire wide/survey scans was at 160 eV pass energy using a hybrid lens in the slot mode. The centre used for the scans was at 520 eV and the width at 1205 eV, with steps at 1 eV and dwell times at 300 ms. For the high resolution scans, the resolution was changed to 10 eV pass energy in the slot mode.

xii. The Brunauer-Emmett Teller (BET) method was employed to determine surface area and porosity. Nitrogen adsorption/desorption isotherms were measured at 77 K using a Micromeritics ASAP 2020 Surface Area and Porosity Analyzer. Prior to each measurement, degassing was carried at 90ºC for four days. The BET surface area and total pore volume were calculated from the isotherms obtained.

2.3 Syntheses

2.3.1 SiNPs-NH_2, Scheme 3.1

Unfuctionalized silica nanoparticles (SiNPs-OH) were synthesized as reported in literature [**58**]. The unfunctionalized SiNPs-OH were then functionalized with APTES as reported in literature [**79**]. Briefly in a round bottomed flask equipped with a stirrer, 0.3g of SiNPs-OH was added in 3 mL of toluene and 2 mL of APTES was added dropwise and the reaction was allowed to continue for 48 h, afterwhich the SiNPs-NH_2 were precipitated with ethanol and were washed with water for several times.

2.3.2 Tris[(4-(pyridin-4-ylthio)-2- thio-4-methylthiazol-5-yl)acetic acidphthalocyanine] zinc (II) (6), Scheme 3.2

Synthesis of low symmetry MPc was carried out by condensation of phthalonitriles **6a** (0.95 mmol) and **6b** (0.32 mmol) with 0.16 mmol of $Zn(OAc)_2$. The mixture was refluxed at 240°C overnight in n-pentanol (3 mL)in the presence of DBU (0.1 mL) as a catalyst. The product was precipitated using diethyl ether. The product of interest was isolatedusing a silica column with DMF:ethyl acetate (3:1) as an eluting solvent system. A green product was obtained. Yield 25%.CHNS Calc. for ($C_{53}H_{30}N_{12}O_2S_5Zn.H_2O$):C,57.26; H, 22.88; N, 15.12; S,14.40. Found: C, 56.98; H, 2.67; N,14.67; S, 13.57. ^{1}H NMR (600 MHz, DMSO) δ 9.08 (s, 1H, O-H), 8.55 (d,5H, Ar-H), 8.28 (dd, 3H,Ar-H), 7.98 – 7.59 (m, 11H,Ar-H), 7.49 – 7.10 (m, 5H, Ar-H), 2.96 (s, 2H, CH_2), 2.75 (s, 3H, CH_3). IR (ATR): v(cm^{-1})2849-2916(Ar-C-H stretch), 1088-1037 (-C-O stretch), 1718-1605(-C=O), 3827 -3046 (O-H), 898 -825 (-C-S-). Maldi-TOF Calculated m/z =1092.59; Found m/z = 1090.59 $[M-2]^+$. λ_{max} nm (log ε) DMSO 686 (4.95),623 (4.27), 361 (4.57).

2.3.3Chloro (2,9,16(2,9,17))-tris-(tert-butylphenoxy) subphthalocyanine boron (II) (7) and N, N-dimethyl-3-(1-oxidanyl)propan-1-amine (2,9,16(2,9,17))-tris-(tert-butylphenoxy) subphthalocyanine boron (II) (8), Scheme 3.3

Tert-butylphenoxyphthalonitrile **7a**, (100 mg, 36.21 mmol) under argon was suspended in 1mL *p*-xylene. BCl_3 (1M) was quickly added in the reaction vessel and the reaction was stirred at room temperature for 30 minutes after which the temperature was increased to 150^oC for 3 h. A pink product (complex **7**) was isolated then purified over silica column chromatography to remove unreacted and by-products using ethyl acetate and hexane in 1:1 as an eluent. Yield 23.1%.$C_{54}H_{49}BClN_6O_3$Calc:C, 74.10: H, 5.53; N, 9.60. Found: C, 74.04; H, 5.75; N, 9.59.^{1}H NMR (300 MHz, DMSO-d_6) δ 8.08 (d,3H, Ar-H), 7.76 (d,3H, Ar-H), 7.51 (d, 6H, Ar-H), 7.33 (d,3H, A-r-H), 7.12 (d,6H, Ar-H), 1.31 (s, 27H,C-H).IR (ATR): v(cm^{-1}):3071 (Ar-C-H), 2960-2869 (C-H), 2257 (C=N), 1275-1167 (C-N), 1089-1020 (C-O-C), 760-655(B-Cl). Maldi-TOF Calculated m/z =876.27, found = 875.33$[M-1]^+$. λ_{max} nm ethanol (log ε):567 (4.91),513 (4.40), 340 (4.49).

In a reactor flask equipped with a magnetic stirrer, complex **7** (100 mg, 91.4 mmol, 1 equiv) and 3-dimethylamino-1-propanol (3.66 mmol, 4 equiv) were added. Dry toluene (3mL) and pyridine (1mL) were then added, the reaction proceeded at 120^oC for 24h. The solvents were then removed under pressure in a rotary evaporator. A violat product (complex **8**) was isolated. Yield 45%. $C_{59}H_{61}BN_7O_4.H_2O$ Calc: C, 73.69; H, 6.34; N, 10.19. Found: C, 73.87; H, 6.48; N, 9.71. ^{1}H NMR (300 MHz, DMSO-d_6) δ 8.37 (s, 3H,Ar-H), 8.14 (d, 3H, Ar-H), 7.83 (m, 2H, Ar-H), 7.57 (d,5H, Ar-H), 7.40 (d, 3H, Ar-H), 7.18 (d, 5H, Ar-H), 2.15 (s, 12H,R-H), 1.37 (s, 27H, R-H).IR

(ATR): v(cm^{-1}): 3306-3071 (Ar-C-H), 2956-2866 (C-H), 2364-2227 (C=N), 1275-1167 (C-N), 1080-1016 (C-O-C),872-833 (B-O). Maldi-TOF calculated m/z=942.97, found m/z= 941.51$[M+1]^+$. λ_{max} nm ethanol (log ε):567 (4.21), 507 (3.72), 348 (4.35).

2.3.4 Synthesis of SiNPs-OH doped with MPcs, Scheme 3.4

SiNPs-OH were functionalised with complex **1-4** and **6** using the micro-emulsion method as reported in literature [**58**]. Briefly, to a round bottomed flask equipped with a stirrer, a mixture of Triton X-100 (1.8 mL), hexanol (1.8 mL), cyclohexane (7.5 mL), water (400 µL), and 25% NH_3(60 µL) was added, followed by stirring for 30 min. Then, complexes **1-4** and **6**, (15 mg) in DMF (100 µL) were added to the flask and the mixture was stirred for a further 10 min after which 200 µL of TEOS was added. The reaction was allowed to continue for 24 h. The products were isolated with isopropanol via centrifugation, and were washed with ethanol, water and then dried under vacuum. SiNPs without complexes **1-4** and **6** were also synthesized as above.

2.3.5 Conjugation of 6 to SiNPs-NH_2, Scheme 3.5

The carboxylic group on **6** was activated following procedures that have been reported [**80**].Briefly (3.2 mg, 0.002 mmol) of **6** in DMF, DCC (17 mg,0.082 mmol) and (10 mg, 0.082 mmol) DMAP were stirred for 48 h at ambient temperature after which SiNPs (11.2 mg) in DMF were added in the reaction vessel and was further stirred for 48 h. The conjugate was precipitated by methanol and was further washed with methanol, water and was dried in a fumehood. The conjugated MPc is represented as **6**-SiNPs (linked) and the doped above as **6**-SiNPs (doped).

List of publications

1. S. Peteni, K. E. Sekhosana, J. Britton, T. Nyokong, Effects of charge on the photophysicochemical properties of zinc phthalocyanine derivatives doped onto silica nanoparticles, Polyhedron, 138 **(2017)**, 37-45.
2. S.Peteni,T.Nyokong, Enhanced singlet oxygen generation by a low symmetry zinc phthalocyanine when conjugated to silica nanoparticles, InorganicaChimica Acta, Submitted.

Results and discussion

3. Syntheses and characterization.

4. Photophysical and photochemical properties.

Comment:

*The metallophthalocyanines (MPcs) reported in this thesis were synthesized with the aim of doping onto SiNPs via the micro-emulsion method, and conjugating **6** to SiNPsfunctinalized with an amino group. An attempt to dope **5** to SiNPs was done with no success, due to the nature of the substituents (will be discussed in detail later). No attempt was made for doping SubPcs to SiNPs*

3.1 Syntheses and characterization of SiNPs alone

SiNPs-OH were synthesised via micro-emulsion method as reported in literature [**58**]. Functionalization of SiNPs-OH with 3-aminopropyltriethoxysilane to give SiNPs-NH_2 was also done as reported in literature [**79**], as shown in **Scheme 3.1**.

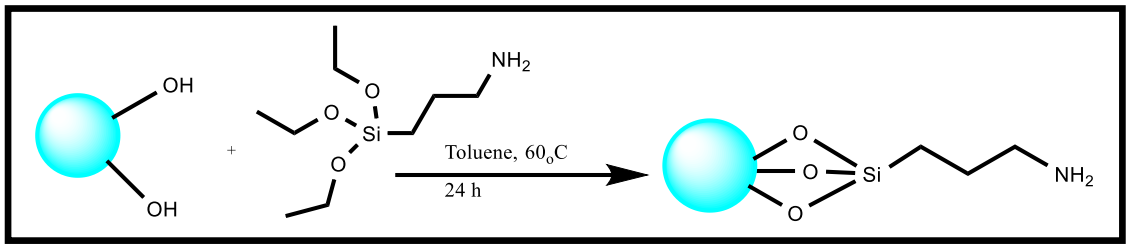

Scheme 3.1: Functionalization of SiNPs-OH to SiNPs-NH_2

The size and morphology of the nanoparticles studied was assessed using transmission electron microscope (TEM). The images of SiNPs-OH and SiNPs-NH_2 are shown in **Figure 3.1**(**A**) and (**B**), respectively. Both SiNPs showed spherical shaped NPs, with no aggregation observed, their average sizes are summarized in **Table 3.1**.

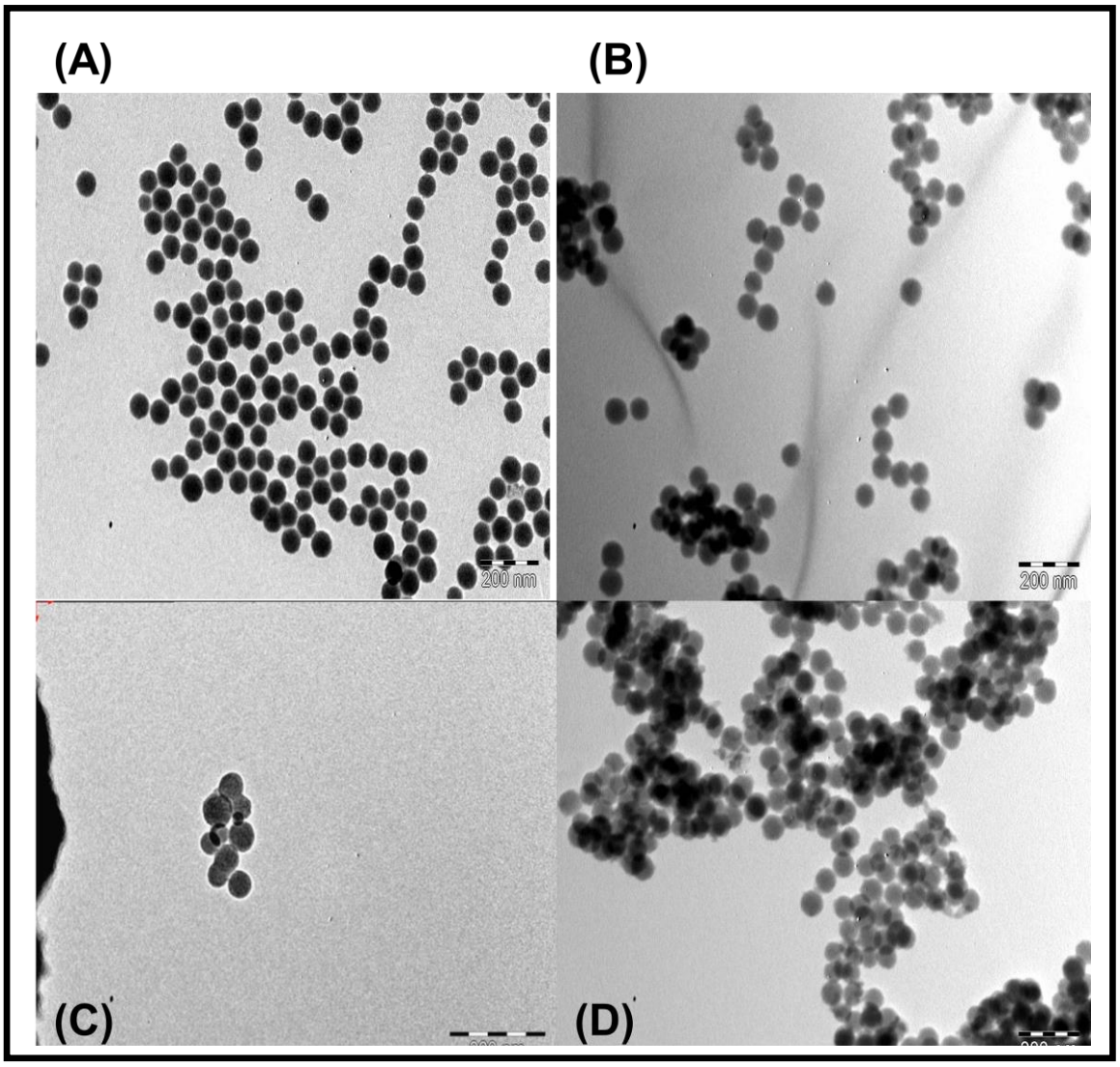

Figure 3.1: TEM micrograms of SiNPs (**A**) SiNPs-OH, (**B**) SiNPs-NH_2 (**C**) **1**-SiNPs, and (**D**) **6**-SiNPs (linked).

Table 3.3: Averages sizes of NPs and conjugates

NPs/ Conjugate	Average sizes (nm)
SiNPs-OH	55
SiNPs-NH_2	59
1-SiNPs	67
2-SiNPs	68
3-SiNPs	73
4-SiNPs	68
6-SiNPs (linked)	69
6-SiNPs (doped)	69

FTIR was used to determine the functional groups onSiNPs. **Figure 3.2** shows theFT-IR spectra of (**A**) SiNPs-OH and (**B**) SiNPs-NH_2. A dominant siloxane peak at approximately 1100 cm^{-1} was observed for both SiNPs-OH and SiNPs-NH_2. A broad O-H stretch was observed at 3500-3000 cm^{-1} for SiNPs-OH upon which after functionalization, the O-H peak disappeared. A decrease in intensity of Si-O-Si peak was observed which could indicate that functionalization occured, as well as a weak N-H peak at approximately 1700 cm^{-1} was observed.

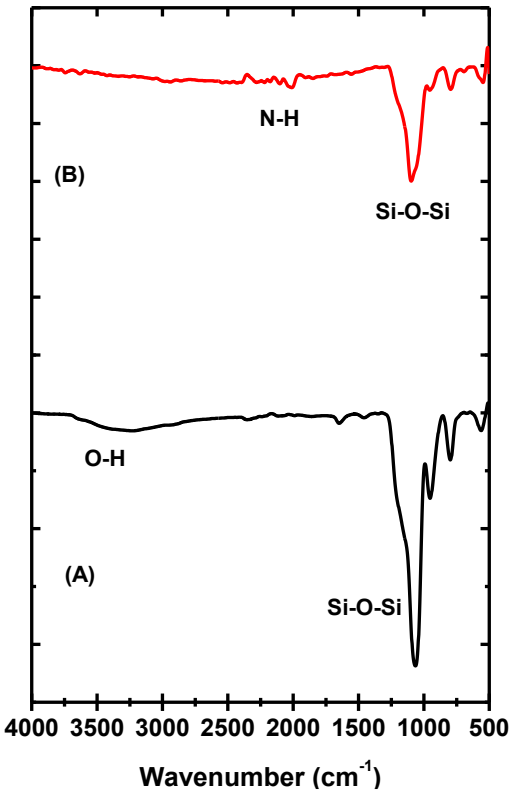

Figure 3.2:FTIR of (**A**) SiNPs-OH and (**B**) SiNPs-NH_2.

X-ray powder diffraction (XRD) was employed to provide information about the nature of SiNPs nanoparticles synthesized. **Figure 3.3** shows the XRD diffractogram of (**A**) SiNPs-OH as a representative of SiNPs synthesized. The XRD pattern shows a broad peak at 2θ= 20-30°. A similar pattern was observed for the SiNPs-NH_2. The armophous behaviour of SiNPs has been reported before in literature [**81**, **82**].

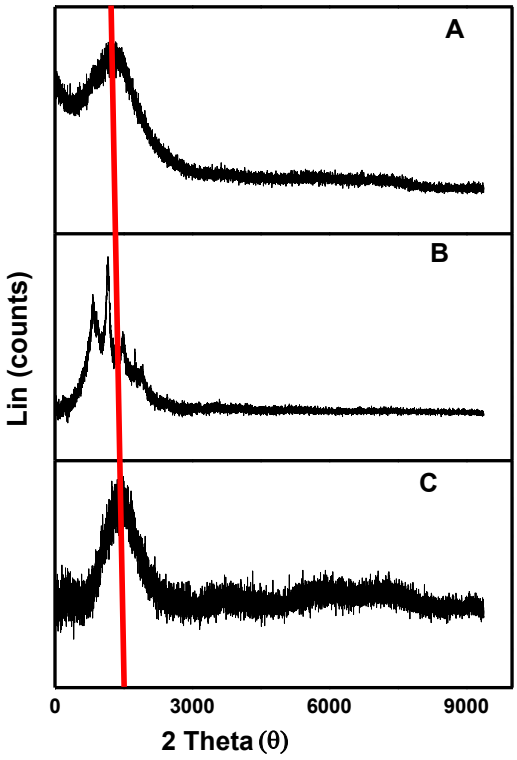

Figure 3.3: XRD of (**A**) SiNPs-OH, (B) **2**, (C) **2**-SiNPs.

3.2 Syntheses and characterization of phthalocyanines and subphthalocyanines

Complexes **1**-**4** and **5** have been reported [**5**, **49**-**51**]. Synthesis and characterization of complexes **6**, **7** and **8** are reported here for the first time. The synthesis of **6** was achieved by the condensation of **6a** and **6b** in the presence DBU as a catalyst, n-pentanol, and $Zn(OAc)_2$ as shown in **Scheme 3.2**.Complex **7** was synthesized via cyclization of **7(a)** in the presence of p-xylene and trichloroboronas shown in **Scheme 3.3**. To displace chlorine which was the axial ligand, **7** was substituted with 3-dimethylamino-1-propanol to yield complex **8**. The synthesized complexes **6**, **7** and **8** were characterized spectroscopically by infra-red (IR), UV-Vis, ^{1}HNMR and mass spectroscopies, as well as elemental analysis.^{1}H NMR spectra showed all the

protons in their correct positions. The absence of the sharp C≡N vibration (~2230 cm^{-1}) in the IR spectra of both Pcs and SubPcs complexes confirmed phthalonitrile cyclization.The found mass to charge ratio for **6** was 1092.05 amu which corresponded to the calculated value, as shown in **Figure 3.4**. ^{1}HNMRspectra for **6** showed the singlet proton of the carboxylic acid end resonating at 9.08 ppm, CH_2 protons resonating at 2.96 ppm as a singlet, and CH_3 protons resonating at 2.75 ppm in the experiment, while the aromatic protons were found between 8.55– 7.10 ppm integrated to give anticipated number of protons.

The formation of **7**, was confirmed with mass spectroscopy where the calculated m/z ratio was 876.27, the found m/z was 875.33 amu. ^{1}HNMR showed a singlet for 27 protons resonating at 1.31 ppm for CH_3 while the aromatic protons resonated between 8.08-7.12 ppm. For **8** the disappearance of B-Cl bond at 760-655 $cm^{-1}$for **7** in the FT-IR spectra with an occurance of a new bond of B-O at 872-833 cm^{-1}confirmed the presence of a new substituted axial ligand, ^{1}HNMR further confirmed the presence of protons resonating for **8** as aromatic protons ranged from 8.37-7.18, 2.15 for 12H due to the presence of the newly substituted axial ligand which were not present in **7**. Elemental analyses for complexes **6, 7, 8** are in agreement with predicted values.

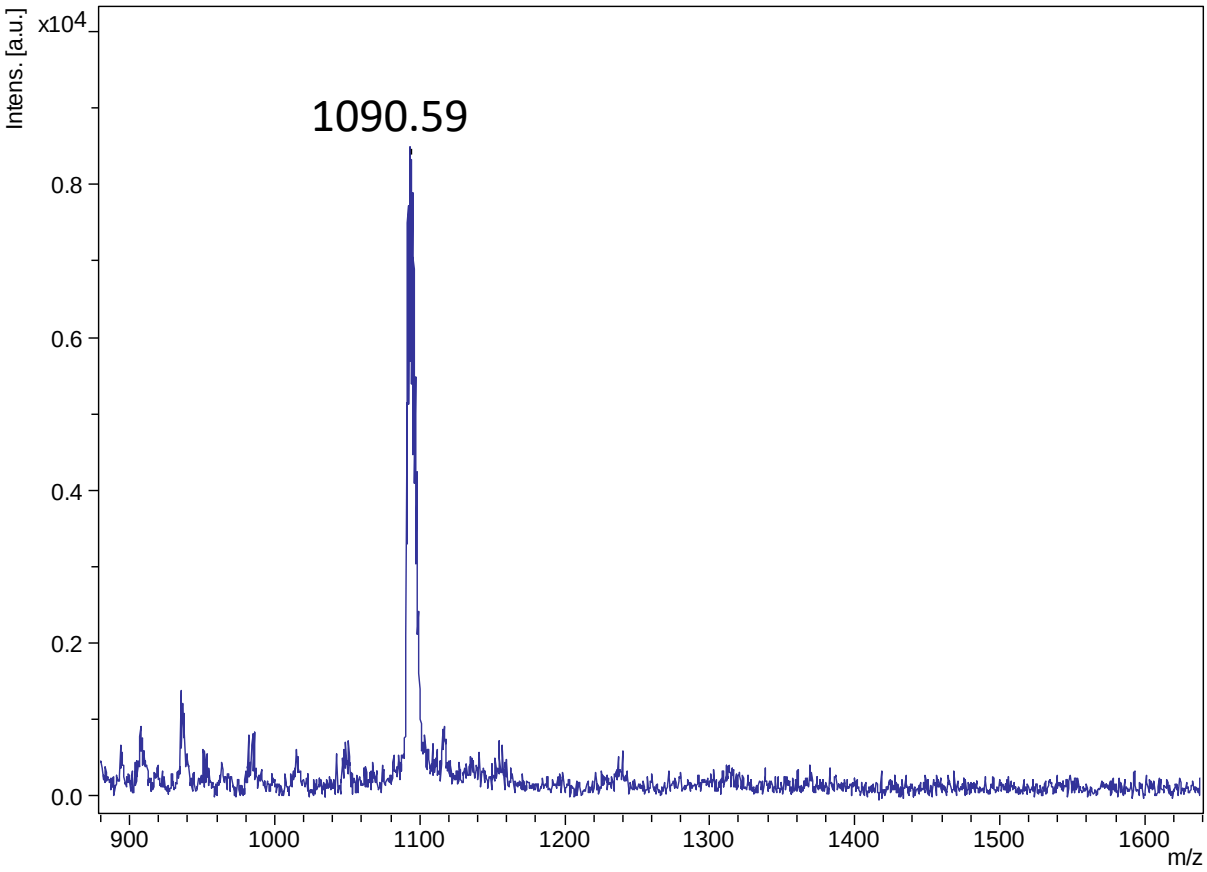

Figure 3.4: Maldi-TOF of complex **6**

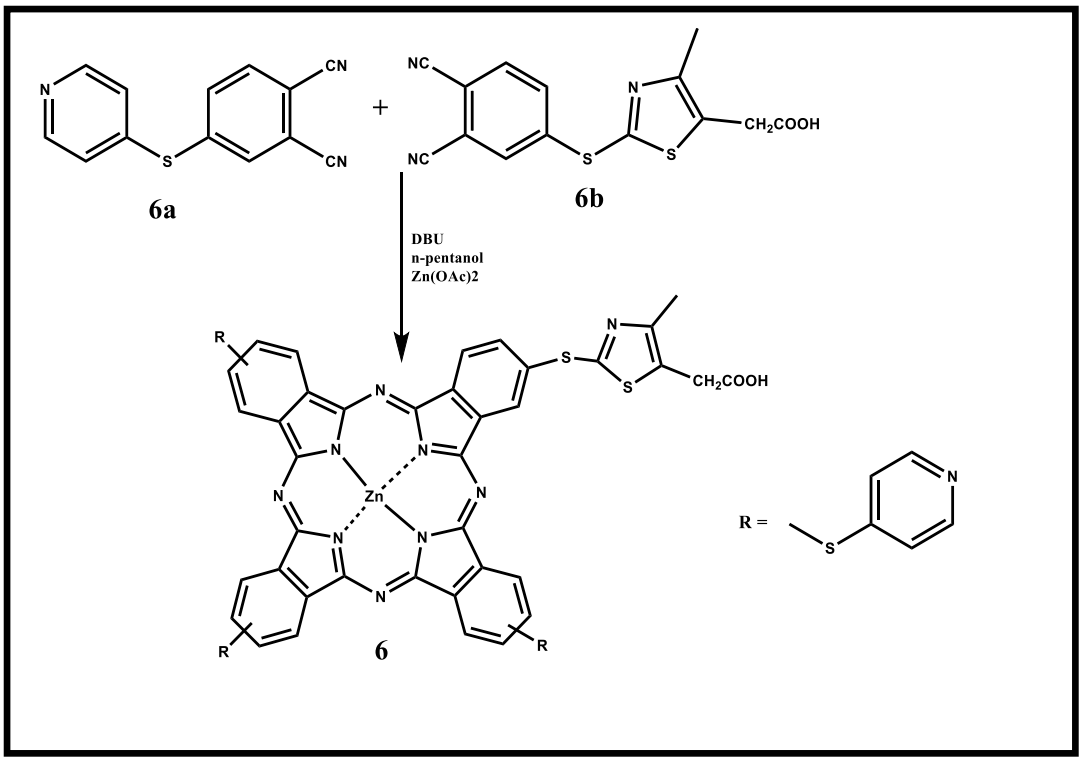

Scheme 3.2: Synthesis route of complex **6**.

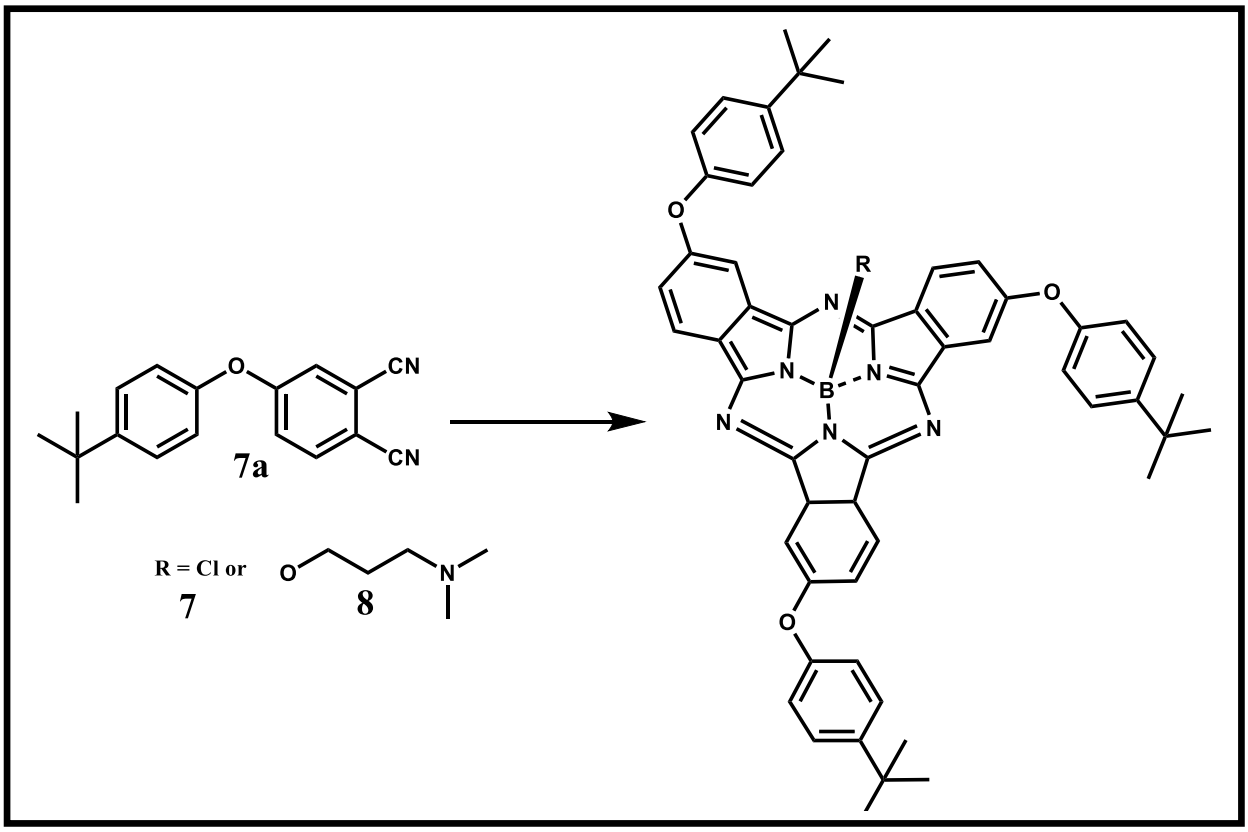

Scheme 3.3: Synthesis route of complex **7**and **8**.Reaction conditions for synthesis of **7**:BCl_3, p-xylene, 180^oC,for **8:** pyridine,toluene, 120^oC.

The UV-Vis spectra of all MPcs and SubPcs are shown in **Figure 3.5**. The ground state absorption spectra showed a monomeric behaviour for all the MPcs and SubPcs which is shown by the sharpness of the Q-band [**83**]. Complex **2** is red shifted compared to complex **1**,due to the presence of electron donating groups (NH_2)which are known to shift the Q-band to the near-IR [**83**], **Table 3.2**. Complex **4** is slightly red shifted compared to complex **3** by 4 nm, **Table 3.2**. The spectrum of complex **5** was recorded in toluene since it was not soluble in DMSO, hence the spectra cannot be compared. Complex **6** has a shoulder near 630 nm which is

typical of H-aggregates [**83**]. Complexes **3** and **4** are hydrophilic but were highly aggregated in water, as can beseen in **Figure 3.5(F)**. Aggregation in phthalocyanines is judged by splitting or broadening of the Q-band as a result of coplanar association of Pc rings progressing from monomers leading to aggregates [**83**]. Aggregation is typical for phthalocyanines in water [**83**]. Monomeric behaviour was observed for both SubPcs (**7** and **8**), with a blue shifted Q-band compared to MPcsdue to its 14π electron system, **Figure 3.5(G)**. The Q-band of **7** is slightly red shifted than**8**. It has been reported that axial substitution does not significantly affect the Q-band of SubPcs, hence the observed shift for **8** [**84**,**85**], **Table 3.2**.

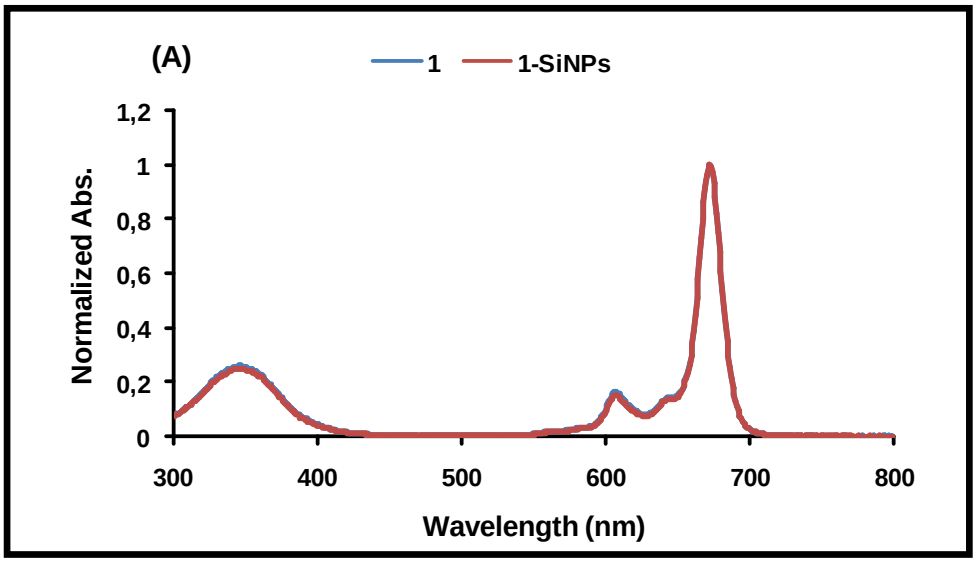

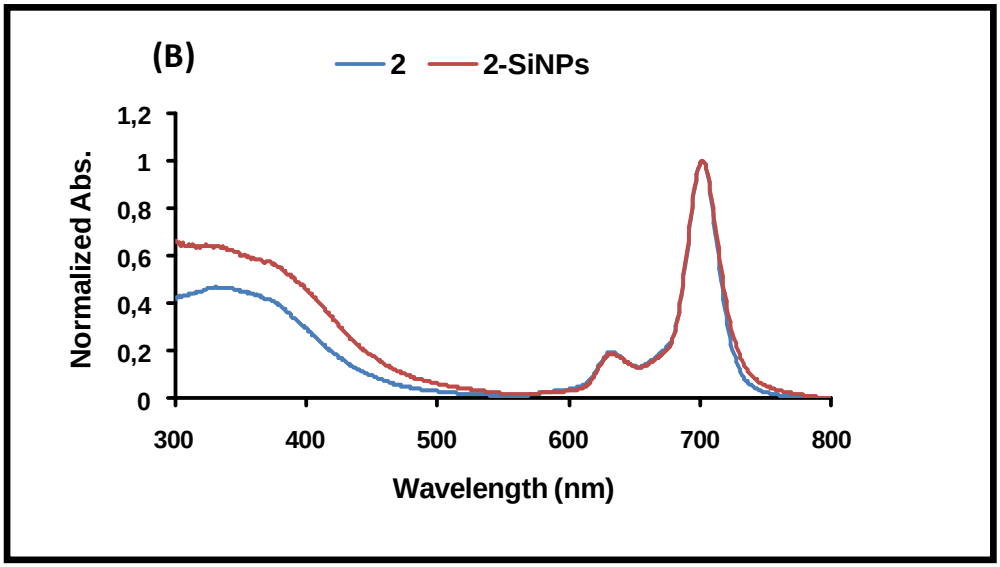
(B)
2
2-SiNPs
Normalized Abs.
1,2
1
0,8
0,6
0,4
0,2
0
300
400
500
600
700
800
Wavelength (nm)

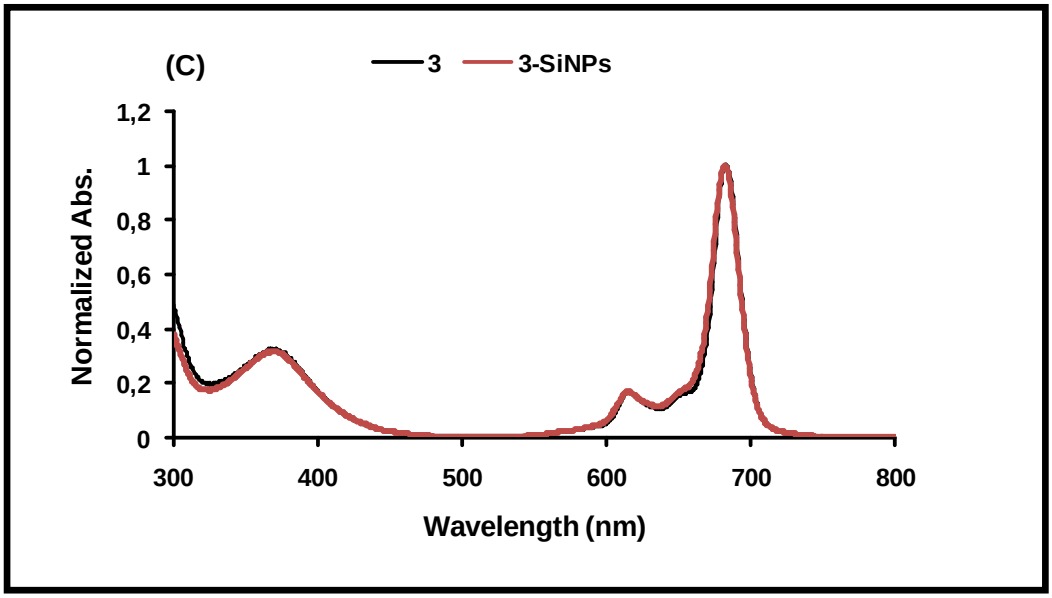
(C)
3
3-SiNPs
Normalized Abs.
1,2
1
0,8
0,6
0,4
0,2
0
300
400
500
600
700
800
Wavelength (nm)

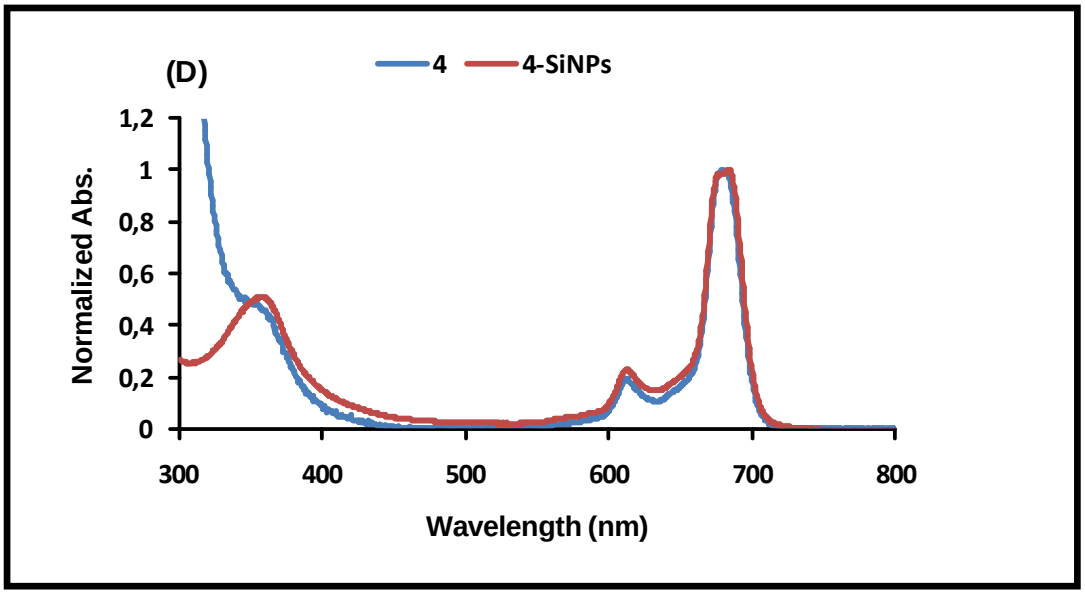
(D)
4
4-SiNPs
Normalized Abs.
1,2
1
0,8
0,6
0,4
0,2
0
300
400
500
600
700
800
Wavelength (nm)

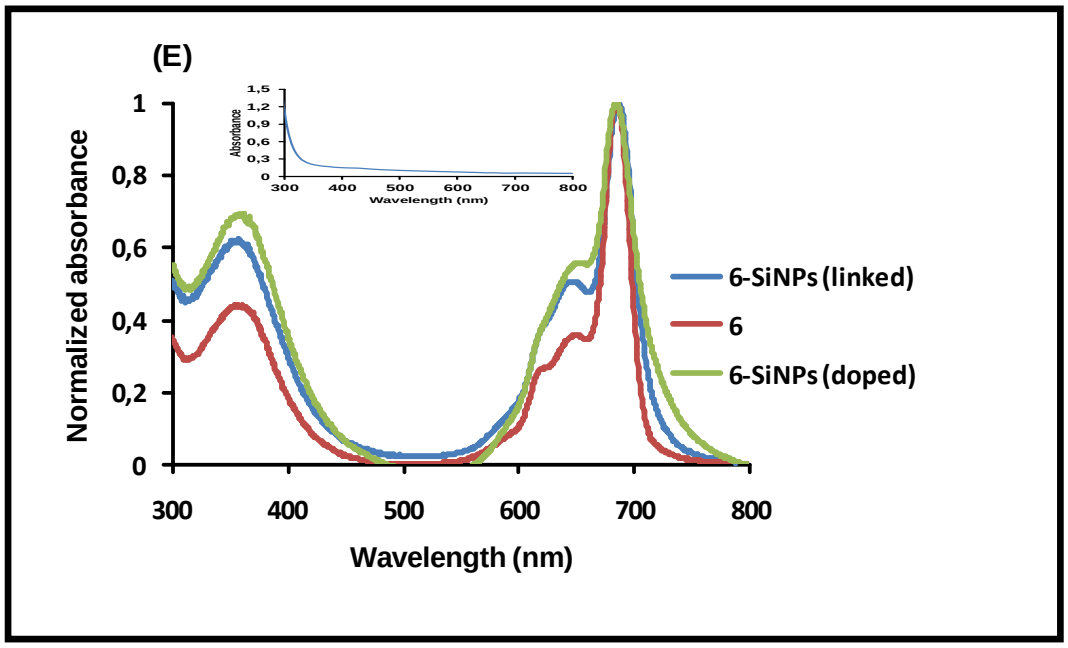
(E)
Normalized absorbance
1
0,8
0,6
0,4
0,2
0
300
400
500
600
700
800
Wavelength (nm)
Absorbance
1,5
1,2
0,9
0,6
0,3
0
6-SiNPs (linked)
6
6-SiNPs (doped)

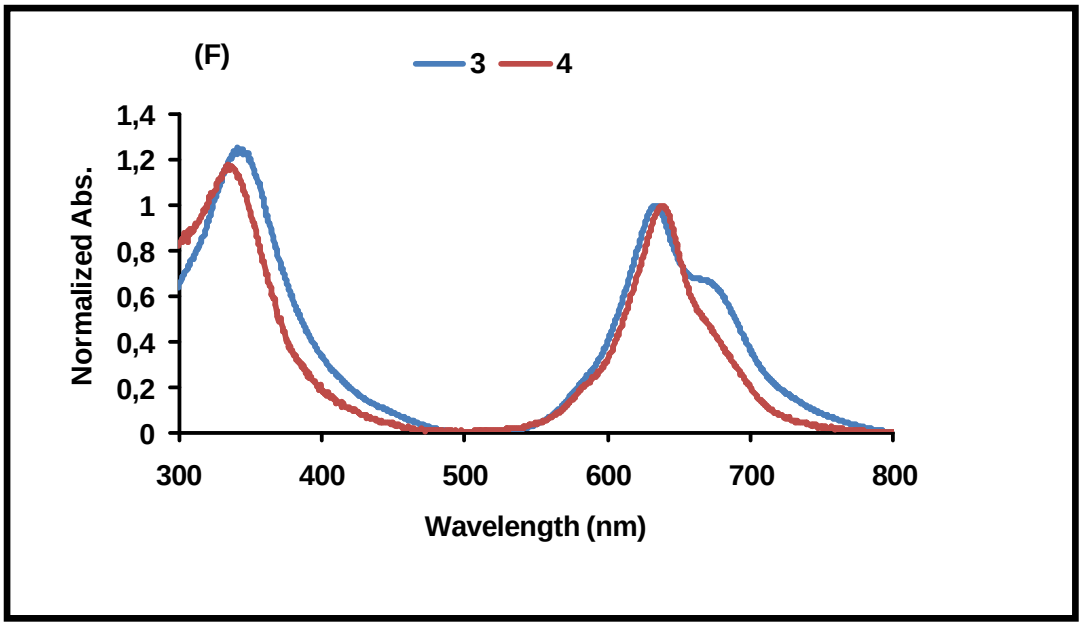

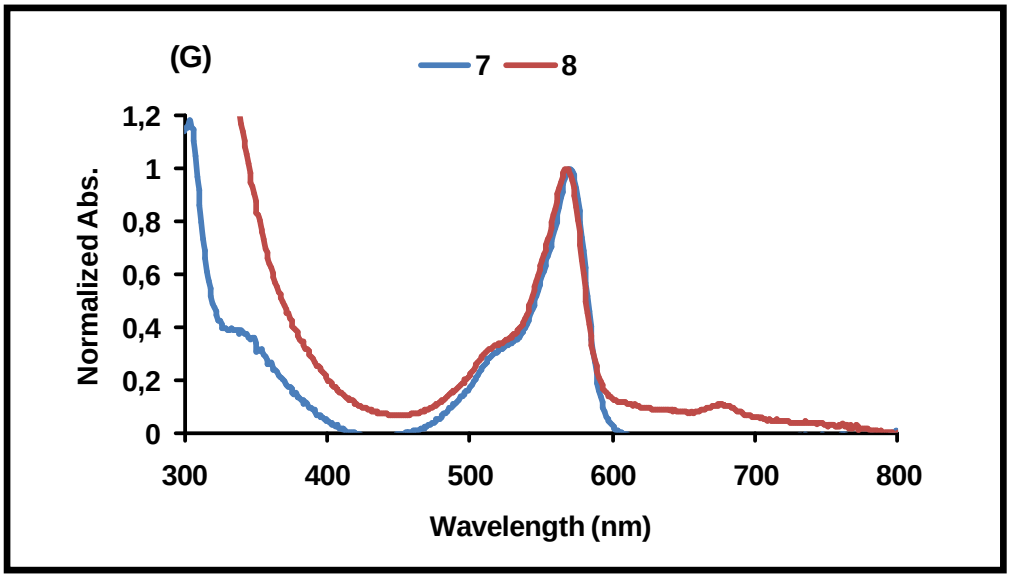

Figure 3.5: Uv-Vis showing (**A**) **1**, **1-SiNPs** (**B**) **2, 2-SiNPs**, (**C**) **3, 3-SiNPs,** (**D**) **4, 4-SiNPs** (**E**) **6, 6-SiNPs (doped), and 6-SiNPs linked in DMSO** in toluene (**F**) **3** and **4** in DMSO:H2O and **(G) 7** and **8** in toluene

Table 3.2: showing Q-band maxima of complexes 1-4, and 6 with their conjugates and complexes 5, 7-8.

Complex/ Conjugate[a]	**Solvent**	**Q-band(nm)**
1	DMSO	670
1-SiNPs (194)	DMSO	670
2	DMSO	686
2-SiNPs (49)	DMSO	686
3	DMSO	683
	Water:DMSO	635
3-SiNPs (10)	DMSO	683
	Water:DMSO	645
4	DMSO	688
	Water:DMSO	638
4-SiNPs (7)	DMSO	688
	Water:DMSO	639
5	Toluene	696
6	DMSO	686
6-SiNPs (linked) (7)	DMSO	685
6-SiNPs (doped) (6)	DMSO	687
7	Ethanol	571
8	Ethanol	567

[a] values in brackets are loading in µg/mg (Pc/SiNPs)

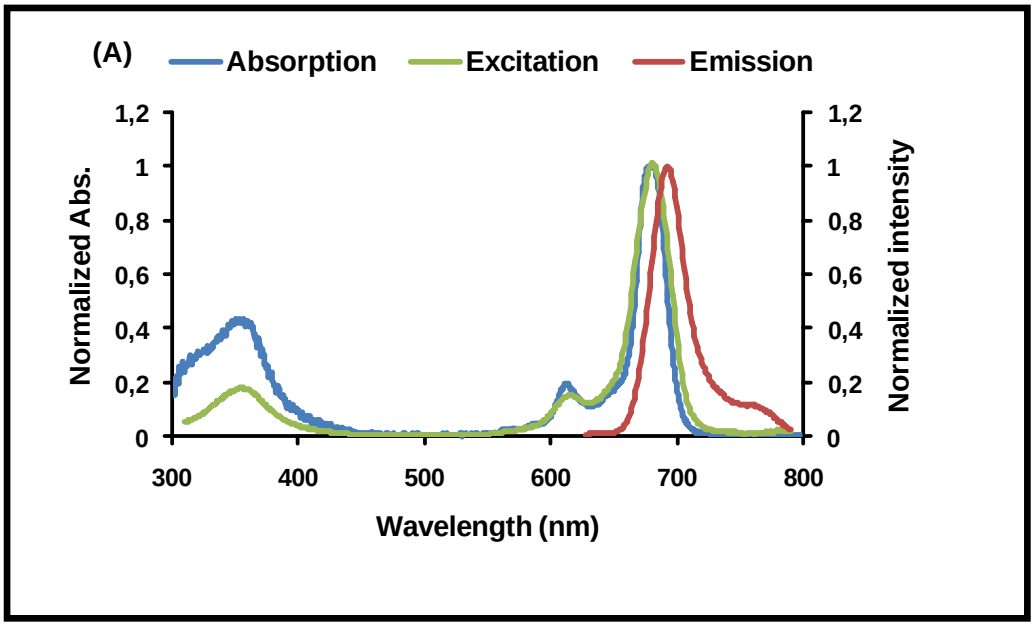
(A)
Absorption
Excitation
Emission
Normalized Abs.
Normalized intensity
1,2
1
0,8
0,6
0,4
0,2
0
300
400
500
600
700
800
Wavelength (nm)

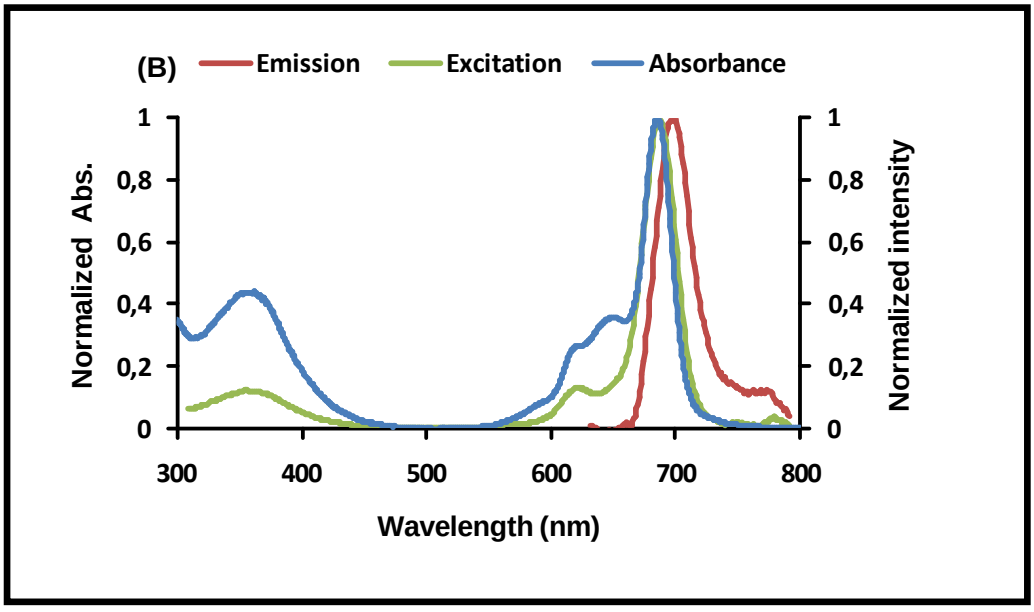
(B)
Emission
Excitation
Absorbance
Normalized Abs.
Normalized intensity
1
0,8
0,6
0,4
0,2
0
300
400
500
600
700
800
Wavelength (nm)

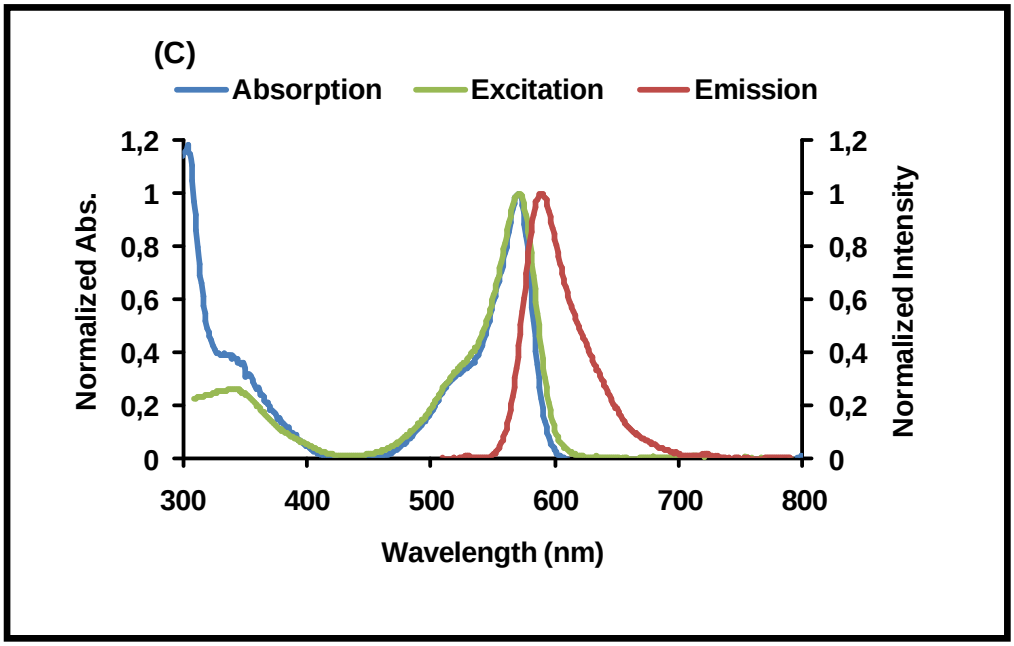

Figure 3.6: Absorption, excitation and emission spectra of (**A**) **4**, (**B**) **6,**in DMSOand (**C**) **7** in ethanol.

The absorption, emission and excitation are shown in **Figure 3.6**. Complex **4** is used as an example for the known MPcs. Emission spectra are mirror images of both the absorption and excitation, meaning the absorbing species is the same as the emitting species. The same was observed for all complexes.

3.3 Interaction of SiNPs with MPcs

3.3.1 Syntheses

The MPcs were readily doped onto SiNPs-OH, as shown in **Scheme 3.4**. Complexes **1** and **2** are hydrophobic while complexes **3** and **4** are hydrophilic. TEOS was used as aSiNPs-OH precursor, TEOS allows for hydrophobic dyes to be dragged in the silica nanoparticles [**86**], hence complexes **1** and **2** can be embedded into the SiNPscore.In addition, since complex **2** contains amino groups, it is expected that

there will be interactions between amino groups of the phthalocyanine and the hanging hydroxyl of the silica core to facilitate the grafting as reported before [**86**]. Positively charged complex **3**, could be electrostatically bonded to negatively charged silica [**58**]. Complex **4** which is negatively charged could suffer repulsions from the negatively charged SiNPs. The encapsulation of complex **1** which contains no ring substituents could be through axial ligation of the dangling hydroxyl groups within the SiNPs. Due to the polar nature of substituents in complex **5**, doping of **5** onto SiNPs-OH was not successful. It has been reported that another silica precursor is required hexadecyltrimethoxysilane (HDTMOS) [**86**], for Pcs with polar substituents to be doped. This was not attempted in this work.

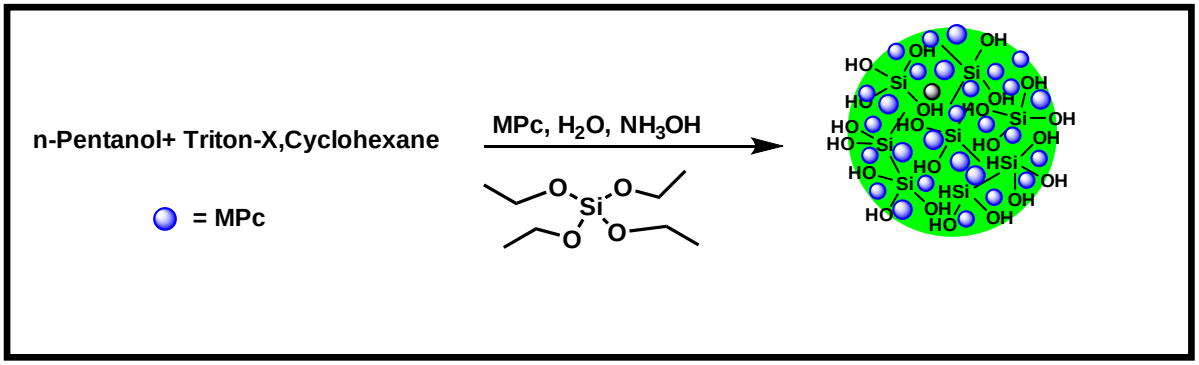

Scheme 3.4: Representation of doping of MPcs onto SiNPs

Complex **6** was linked to SiNPs via the amide bond, DMAP/DCC were employed as coupling agents, after which NH_2 functionalizedSiNPs in DMF were added, **Scheme 3.5.** The conjugates were represented as (without a chemical bond) **6**-SiNPs

(doped)and **6**-SiNPs (linked). Amide bond formation was confirmed by FT-IR (discussed below).

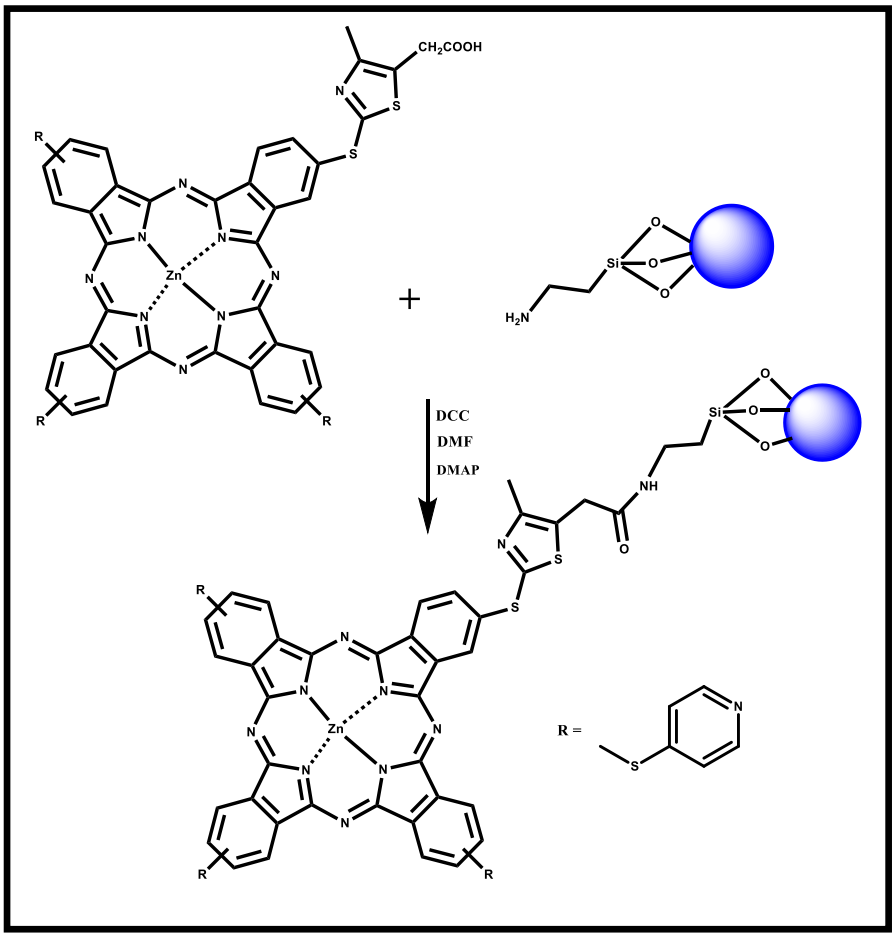

Scheme 3.5: Conjugation of **6** to SiNPs-NH_2.

3.3.2 Ground state absorption and fluorescence spectra

There were no changes in the aborbancesfollowing doping for **1**-SiNPs, and **3**-SiNPs as seen in **Figure 3.5**(**A**). However, for (**B**) **2**-SiNPs, (**D**) **4**-SiNPsand (**E**) **6**-SiNPs (doped) and **6**-SiNPs (linked) a slight enhancement around the B-region of the MPc was observed compared to MPcsalone,this is due to the presence of SiNPs which

are known to absorb around the 400-500 nm region. Conjugates **3**-SiNPs and **4**-SiNPs were not fully water soluble; hence 7% of DMSO was added, Q-band maxima values are summarized in **Table 3.2**, and compared to **3** and **4** alone in DMSO:water.

Figure 3.7 shows absorption, emission and excitation of the conjugates (**A**) **2**-SiNPs used as an example for neutral MPcs and (**B**) **3**-SiNPs used an example for charged MPcs and (**C**) **6**-SiNPs(linked) and (**D**) **6**-SiNPs (doped). The absorption spectra were similar to excitation spectra and both were mirror images of the emission spectra, showing that the emitting species was the same as the absorbing species in DMSO. In water all the spectra were highly affected by aggregation, hence spectra not included.

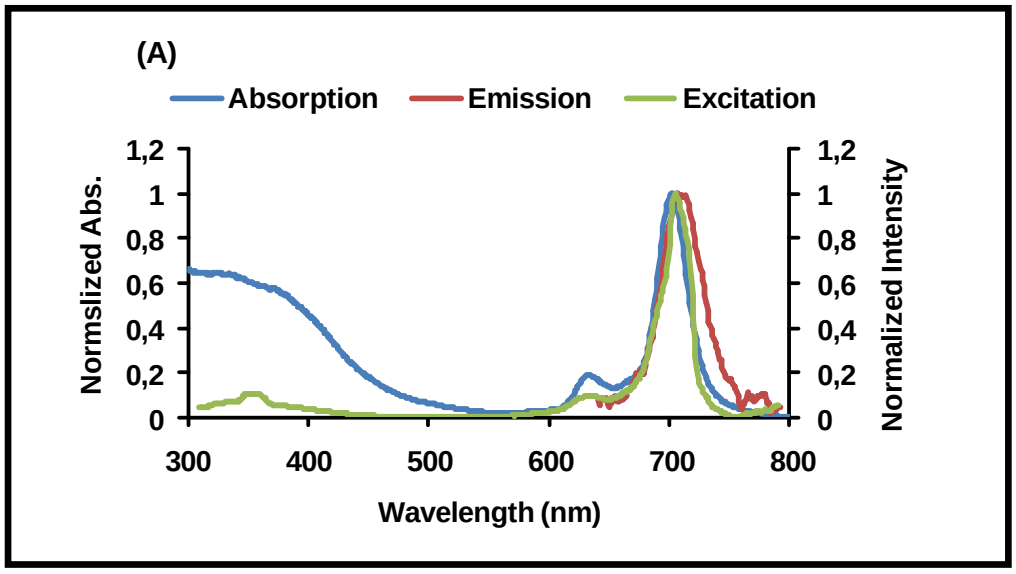

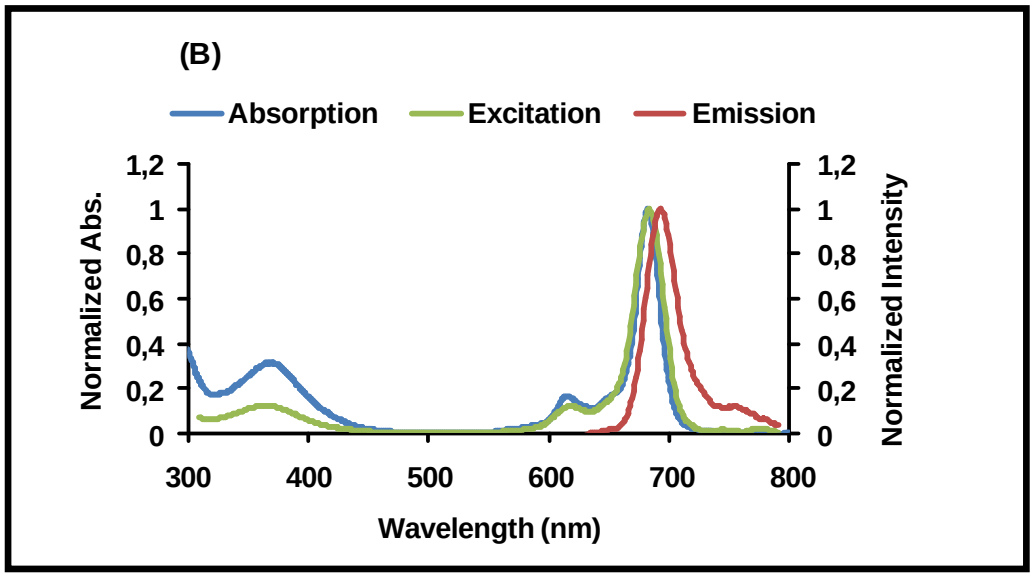
(B)
Absorption
Excitation
Emission
Normalized Abs.
Normalized Intensity
1,2
1
0,8
0,6
0,4
0,2
0
300
400
500
600
700
800
Wavelength (nm)

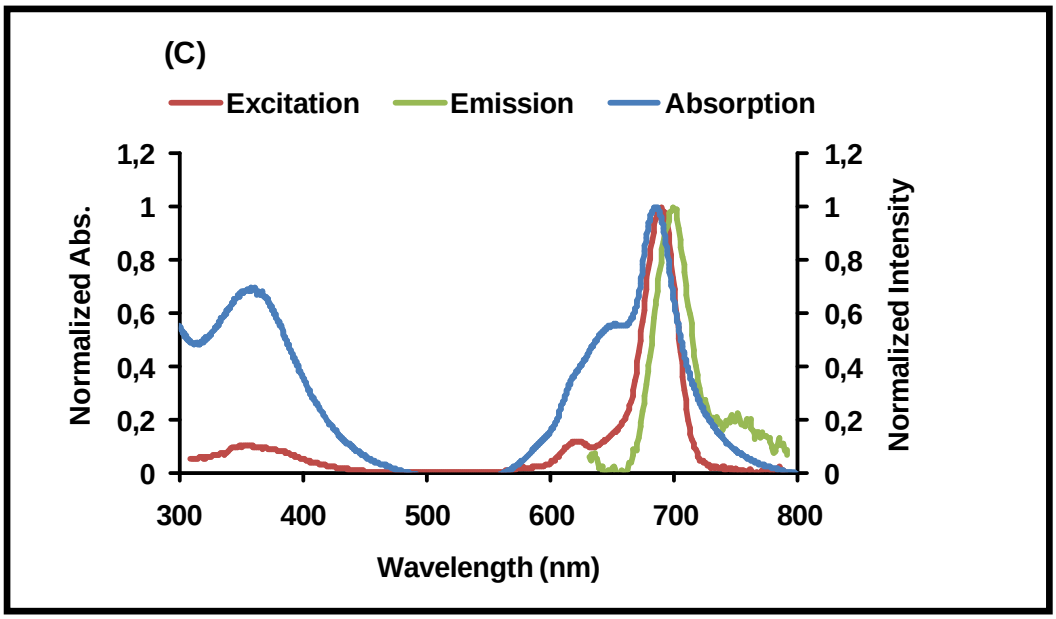
(C)
Excitation
Emission
Absorption
Normalized Abs.
Normalized Intensity
1,2
1
0,8
0,6
0,4
0,2
0
300
400
500
600
700
800
Wavelength (nm)

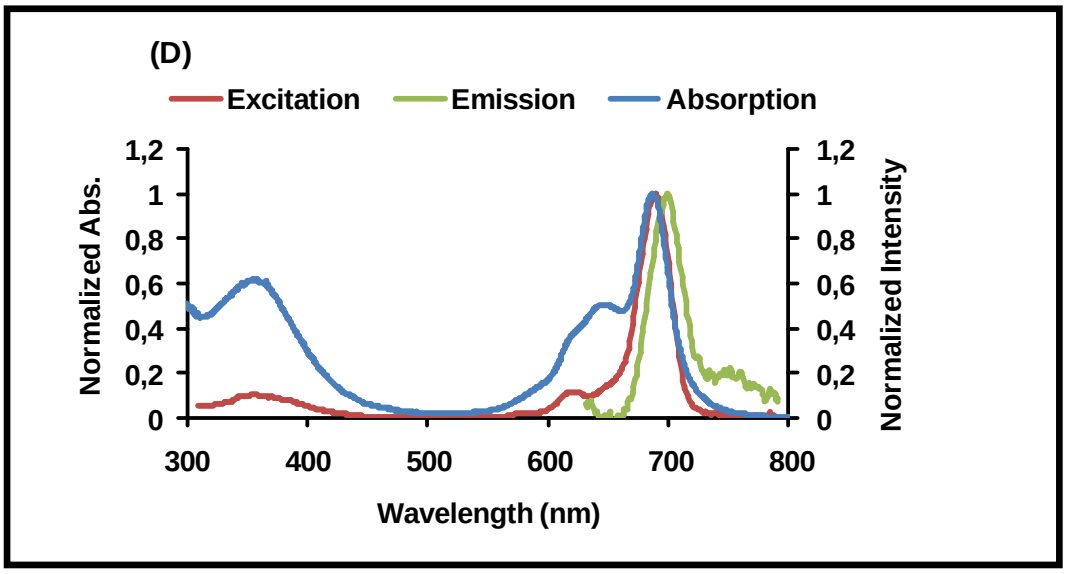

Figure 3.7: Absorption, emission, and excitation of (**A**) **2**-SiNPs, (**B**) **3**-SiNPs, (**C**) **6**-SiNPs (linked) and (**D**) **6**-SiNPs (doped), in DMSO.

3.3.3 Loading capacity

The mass loadings of complexes **1**-**4** and **6** into the SiNPswere determined using UV–Vis of the Pcs using reported methods [**87**-**89**]**.** This involves comparing the Q band absorbance intensities of the conjugateofPcs before and after the conjugation. Equal masses (mg) for Pc and the conjugates were weighed and separately dissolved in the same volume of the solvent. This was followed by comparing the Q band absorbance intensity of the Pcs in the conjugate with that of the initial Pcs before the conjugation. The loadings are listed in **Table 3.2**.

The loading efficiency of the charged MPcs (**3**, **4**) was found to be less than that of the uncharged MPcs.The observed results may be caused by the repulsion which

could be as a result of the negative charge on the surface of SiNPs and that of the MPc in the case of **4**. Since **3** is positively charged maximum loading was expected due to difference in charge, however that was not the case. Loading was found to favour the uncharged MPcs, **1** showed a larger loading compared to **2**.It is possible that hydrophobicity and the lack of bulky substituents could have resulted in easier loading of **1** onto SiNPs. Complex **6** is also neutral and has bulky substituents, however, the loading was low for both linked and doped conjugates. This was surprising since other neutral MPcs showed higher loading.

3.3.4 X-ray Photoelectron Spectroscopy (XPS) and Energy dispersive x-ray spectroscopy (EDS)

To further confirm if doping occurred XPS was used as shown in **Figure 3.8(A)** using SiNPs alone and **2**-SiNP as examples. The XPS survey, **Figure 3.8(A)** showed different binding energies which corresponded to the expected elemental composition.The binding energies and their corresponding elemental composition of the samples are as follows: for SiNPs, Si 2s (100 eV), Si2p (103 eV), C1s (285eV), and O1s (533 eV), while the MPc doped SiNPs showed similar trends as SiNPs alone except for the presence of N1s(396 eV). The MPc doped SiNPsexhibited an increase in %C compared to SiNPs alone, **Table 3.3**, due to the addition of the Pcs. There is a decrease in % oxygen of the conjugates compared to SiNPs alone, **Table 3.3**, even though the Pcs have oxygen which should have resulted in the increase. The observed decrease in % oxygen could suggest that the Pcs are interacting with the hanging hydroxyl on the surface of the SiNPs, hence the large number of hydroxyl are not exposed, the small amount of oxygen atoms on the Pcs are not enough to offset the reduction in % oxygen. The largest reduction in % oxygen was

observed for the positively charged complex **3** which electrostatically binds to SiNPs. In addition, the presence of N is due to MPcs in the doped analogues.

The O1s high resolutionXPSanalysiswas carried out to ascertain the chemical environment of the O1s of the SiNPs and MPcs in the doped analogues, **Figure 3.8(B)**. The O1s spectra for SiNPs was deconvuluted, andonly one peak was observed at 537 eV which corresponded to Si-O-Si (siloxane peak).The O1s spectra of the MPc doped SiNPs (using **3**-SiNPs as an example) accounted for two peaks at 532 eV and 533 eV corresponding to Si-O-Si and C-O-C respectively. C-O-C was due to the MPc macrocycle and their oxo bridge between the ring substituents while Si-O-Si resulted from SiNPs.

(A)

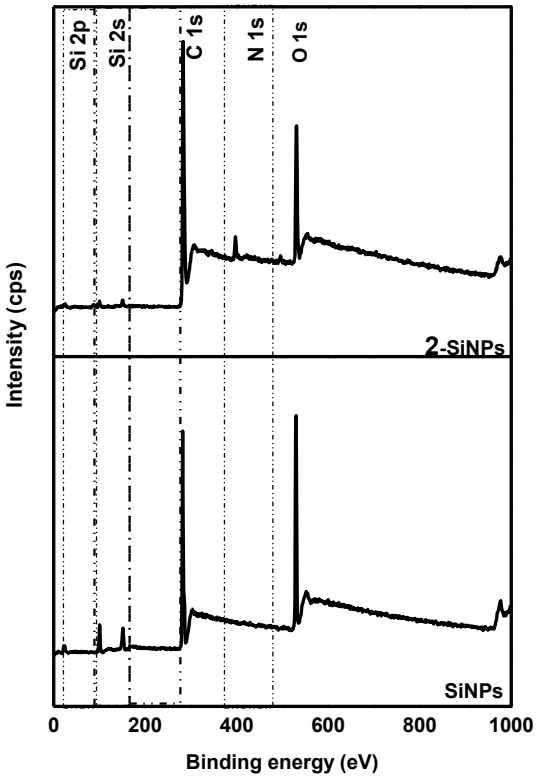

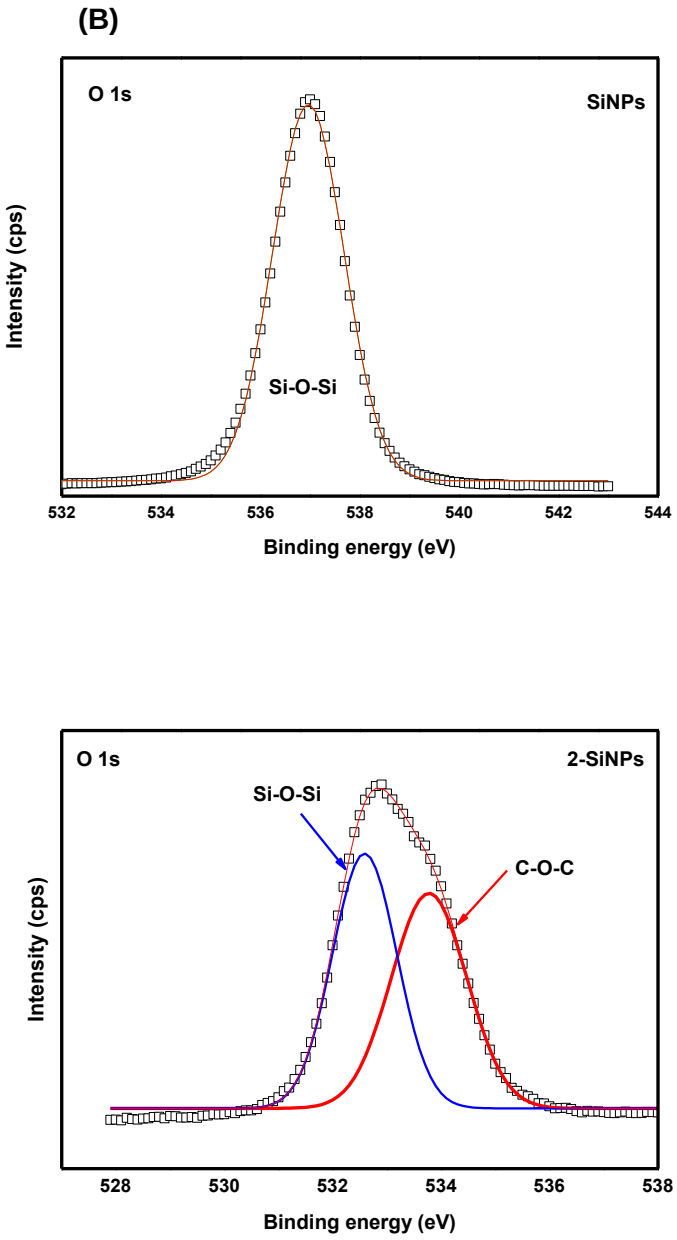

Figure 3.8: XPS spectra (**A**) Wide scan of SiNPs alone and the MPc conjugates and (**B**) O1s High resolution spectra of SiNPs and **2**-SiNPs.

Table 3.3: Elemental composition of conjugates of complexes 1-4

Complex/Conjugate	Atomic concentration (%)					
	C 1s	O 1s	N 1s	S 2p	Na 1s	I 3d
SiNPs	69.05	23.91	-	-	-	-
2-SiNPs	79.88	15.86	1.23	-	-	-
3-SiNPs	79.11	6.05	7.13	-	-	4.93
4-SiNPs	77.06	14.98	0.65	0.53	0.15	-

Quantitative elemental analysis was done using EDX, **Figure 3.9(A)** showing **6** alone and **(B)** **6**-SiNPs (doped). **6** showed the expected elements, following doping/conjugation a new Si peak was observed due to the presence of SiNPs.

(A)

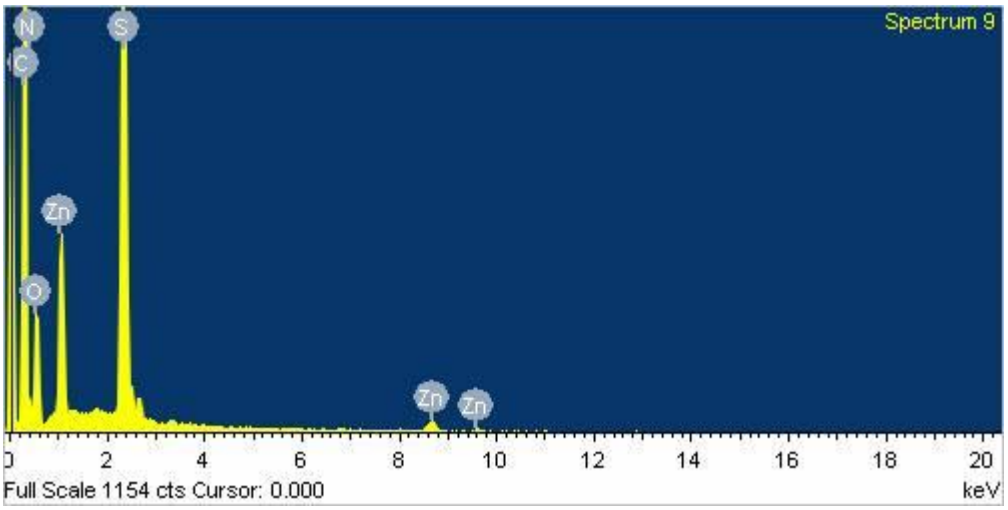

(B)

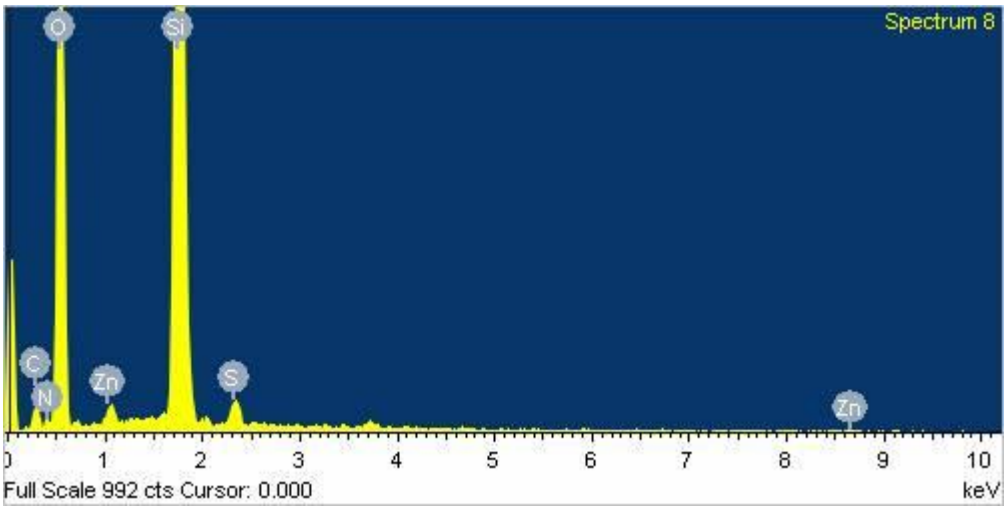

Figure 3.9: Energy dispersive spectra of (**A**) **6** and (**B**) **6**-SiNPs (doped).

3.3.5Transmission electron microscope (TEM)

The morphology and sizesof SiNPs alone and MPc doped or linked SiNPs were investigated by employingTEM as shown in **Figure 3.1**(**C**) for **1**-SiNPs and (**D**) for **6**-SiNPs (linked) (used as examples). There was an increase in size for all doped and linked SiNPs, the average sizesare summarized in **Table 3.1**. The observed increase in sizemay suggest that the dye is enclosed within the matrix of the SiNPs (doped) [**90**]. Also the increase in size could be due to well-known aggregation of Pcs through $\pi\pi$ interactions [**83**].

3.3.6 Brunauer-Emmett-Teller (BET)

BET was performed to determine the pore size, surface area, and nature of doped and undopedSiNPs, **Figure 3.10** ((A) SiNPs-OH alone and (B) **4**-SiNPs used as an example). The isotherms show the partitioning between the gas phase and adsorbed

species as a function of applied pressure. Both the SiNPs alone and the doped SiNPsshowed a type IV isotherm which is typical of mesoporous material [**91**]. The surface area of SiNPs alone was found to be 57.68 m^2/g with a pore size of 27.8 nm and the surface area of **4**-SiNPs was 72.68 m^2/g with a pore size of 9.78 nm. It has been reported that rough surface increases surface area [**91**]. Therefore an increase in the surface of area for **4**-SiNPs may be due to strong surface roughness, which is weaker for SiNPs alone. **4**-SiNPs had a smaller pore size compared to SiNPs alone. The decrease in pore size of **4**-SiNPs is as result of the introduction of MPc onto the surface of the SiNPs.

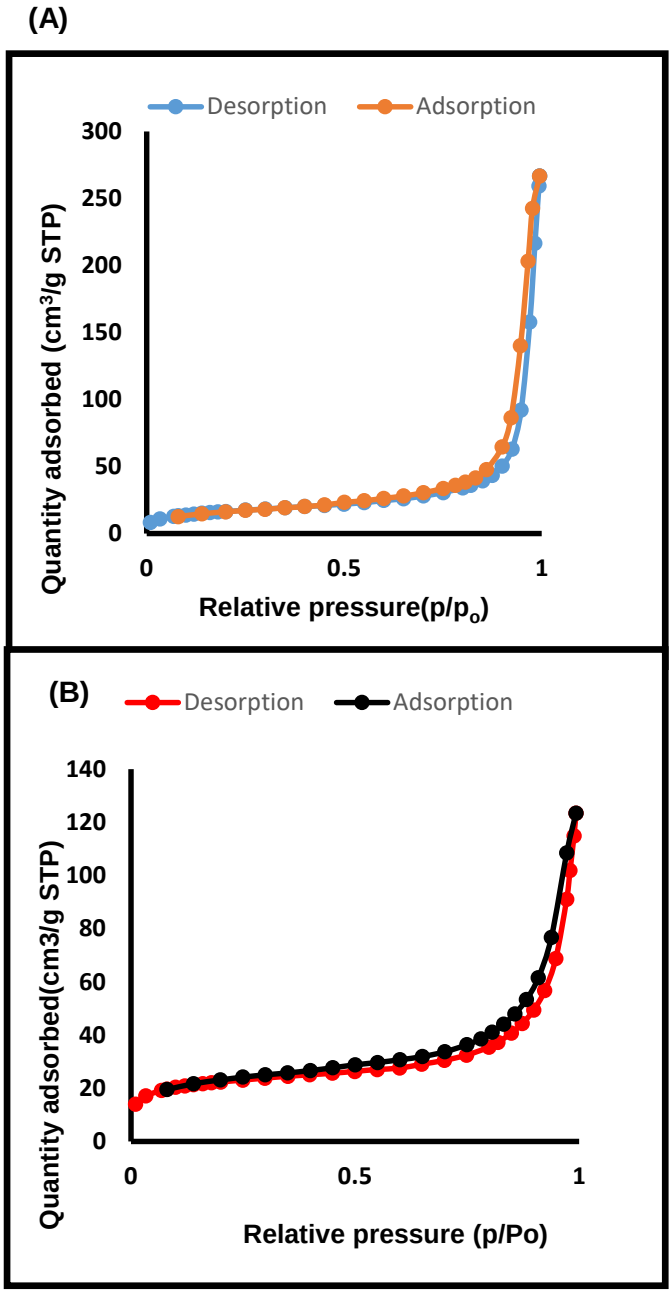

Figure 3.10: Nitrogen adsorption-desorption BET isotherms of (**A**) SiNPs-OH and (**B**) **4**-SiNPs.

3.3.7 Fourier Transform Infrared(FTIR) and X-ray power diffraction (XRD)

To further confirm the doping/conjugation of MPcs to SiNPs FTIR spectra was used. **Figure 3.11** shows the FT-IR spectra of (**A**) SiNPs-OH, (**B**) **2** and (**C**) **2**-SiNPs (used

as examples) for known MPcs. A peak was observed near the 1100 cm^{-1} region due to Si-O-Si stretching for both the SiNPs alone and **2**-SiNPs. For the latter, there were no characteristic peaks due to MPc observed due to the large amount of SiNPs. The same behaviour was observed for all the doped conjugates.

Figure 3.12 shows the IR of (**A**) SiNPs-NH_2, (**B**) **6**, (**C**) **6**-SiNPs (linked) and (**D**) **6**-SiNPs (doped). SiNPs-NH_2 showed a peak at 1092 cm^{-1} which is due to siloxane groups. Complex **6** alone showed a broad OH peak between 3007-3500 cm^{-1}, a C-H stretch at 2875 cm^{-1}, a C-O stretch at 1648-1692 cm^{-1}. Both conjugates (doped and linked) were mainly dominated by the siloxane peaks at 1092 cm^{-1}, however an amide peak at 1648 $cm^{-1}$was observed as seen in the insert, confirming a chemical linkage between **6** and SiNPs-NH_2.

XRD was used to determine the morphology of SiNPs-OH and its conjugates. The XRD pattern of complex **2** alone (**Figure 3.3 (B)**) contains a broad peak between 2θ = 10 and 30°, which is typical of phthalocyanines [**92**]. The embedded sharp peaks suggest some crystalline behaviour, which has been reported before [**93**]. Diffraction pattern of SiNPs alone and of the conjugates showed an amorphous behaviour as shown in **Figure 3.3(A)** and **(C)**. This therefore suggests that the conjugates were mainly dominated by SiNPs as reported before [**68**]. A slight shift in the 2θ value for the conjugate when compared to SiNPs alone was observed. The shift may be due to the formation of a new crystal after conjugation occurred [**93**].

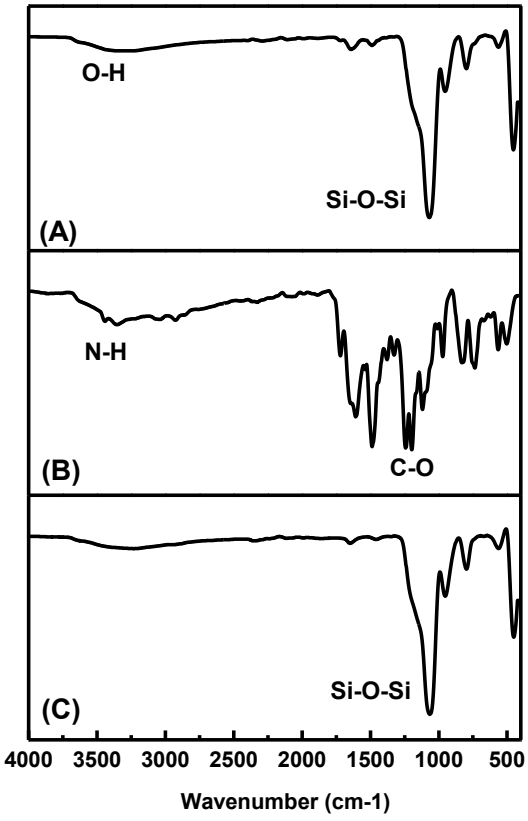

Figure 3.11: FTIR of (**A**) SiNPs-OH, (**B**) **2**, (**C**) **2**-SiNPs.

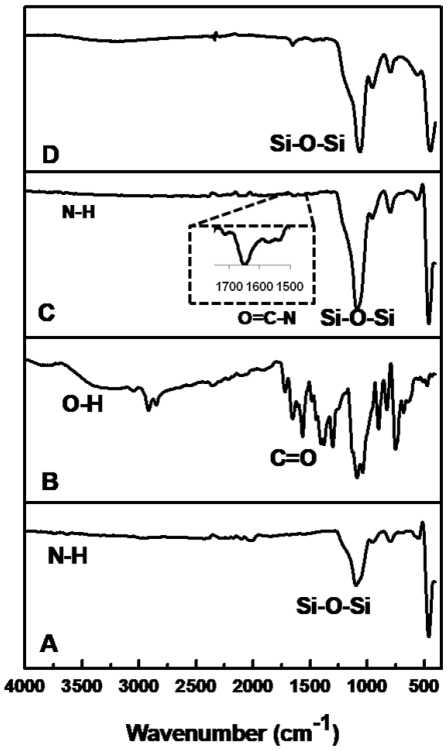

Figure 3.12: (**A**) SiNPs-NH_2, (**B**) **6**, (**C**) **6**-SiNPs (linked) and (**D**) **6**-SiNPs (doped).

3.4 Conclusions

*MPcs bearing different charges (**1**-**4**) (neutral, negative and positive) were readily doped to SiNPs. A low symmetry Pc (**6**) was both conjugated via amide linkage and doped onto SiNPs. Various methods were used to prove if doping/conjugation occurred. Some changes were observed following doping/conjugation. Doping of **5** onto SiNPs was unsuccessful as stated earlier. For SubPcs **7** and **8** only UV-Vis/ fluorescence behaviour are reported.*

Chapter Four

Photopysico-chemical studies

The photophysical and photochemical properties of the synthesized MPcsare discussed. For the MPcs, comparisons are made with respect to the presence of different substituents, and interaction with SiNPs in MPc-SiNPs conjugate. The studies were conducted in dimethyl sulfoxide (DMSO) for **1**-**4** and **6**. Since complex **5** and **7**-**8** were not soluble in DMSO, toluene and ethanol were used, respectively.

Table 4.1: Physicochemical properties of complexes 1-4, and 6 and their conjugates and of 5, 7-8 alone

Complex/ Conjugate	**Solvent**	ϕ_F **±0.01**	ϕ_T	ϕ_Δ **±0.02**	$\tau_F(ns)$	$\tau_T(\mu s)$
1	DMSO	0.20[a]	0.65[b]	0.67[c]	2.8	350[b]
1-SiNPs	DMSO	0.19	0.76	0.47	3.2	244
2	DMSO	0.06[d]	0.51[d]	0.35[d]	2.8[d]	315[d]
2-SiNPs	DMSO	0.01	0.35	0.29	2.6	237
3	DMSO	0.17	0.73	0.41	2.7	326
	Water:DMSO	<0.01	-	0.28	-	-
3-SiNPs	DMSO	0.17	0.87	0.59	2.6	248
	Water:DMSO	<0.01	-	0.37	-	-
4	DMSO	0.17	0.89	0.43	3.0	466
	Water:DMSO	<0.01	-	0.24	-	-
4-SiNPs	DMSO	0.18	0.82	0.80	2.9	519
	Water:DMSO	<0.01	-	0.36	-	-
5	Toluene	0.14	-	0.12	2.57	
6	DMSO	0.09	0.69	0.67	2.57	247
6-SiNPs (linked)	DMSO	0.08	0.85	0.80	2.57	147
6-SiNPs (doped)	DMSO	0.05	0.41	0.25	2.49	233
7	Ethanol	0.22	-	0.52	2.76	-

8	Ethanol	0.19	-	0.83	1.73	-

[a] from reference [**38**], [b] from reference [**44**],[c] from ference[**47**], [d] from reference [**94**]

4.1 Fluorescence quantum yield and lifetimes

All samples and standards were excited at the same wavelength. The absorbances of the solutions at the excitation source were about 0.05 to avoid any filter effects.The fluorescence decay curve is shown in **Figure 4.1** (**2**-SiNPs used as an example). The fluorescence quantum yields were determined using equ.1.1.

The fluorescence quantum yields of **1**and **2** are known as 0.2 and 0.06 in DMSO, respectively [**38, 94**]. The ϕ_F value for complex **2** alone is low due to the known quenching effect of the amino groups [**95**]. Complexes **3** and **4** had equal ϕ_F values, **6** had low ϕ_F maybe due to heteroatomic effect caused by the presence of sulphur [**96**]. Following doping of **1** onto SiNPs there were no significant changes in fluorescence quantum yield. This was also the case with complexes **3** and **4**, but not complex **2, Table 4.1**. Compared to **6** there was no significant decrease for**6**-SiNPs (linked), but a significant decrease in Φ_F for**6**-SiNPs (doped) was observed,**Table 4.1**. It has been reported that when phthalocyaninesare grafted on the surface of theSiNPs, the fluorescence process is more efficient than when not on the surface [**97**], hence the large ϕ_F is observed for **6**-SiNPs (linked) compared **6**-SiNPs (doped).In water:DMSO, the ϕ_F values were low due to known quenching of fluorescence by water [**98**]. SubPcs are highly fluorescent material compared to their Pc analogues. Of note is following axial substitution of **7** to give **8**, a decrease in the

fluorescence quantum yield was observed, which could be due to self-quenching of subphthalocyanine rings [**99**].

There were no significant decreases in the fluorescence lifetimes of the MPcs **2**-**4** following doping, with the exception of **1**-SiNPs, where there was a slight lengthening, **Table 4.1.** For **6** a decrease was observed for **6**-SiNPs (doped) compared to **6** alone however, there was no decreasefor **6**-SiNPs (linked). The decrease for **6**-SiNPs (doped) corresponds to the decrease in ϕ_F. It has also been reported that the increase or decrease in fluorescence lifetimes may depend on orientations of the fluorophore [**73**]. A decrease in fluorescence lifetimes for **7** following axial substitution was observed corresponding to the decrease in ϕ_F (**8**).

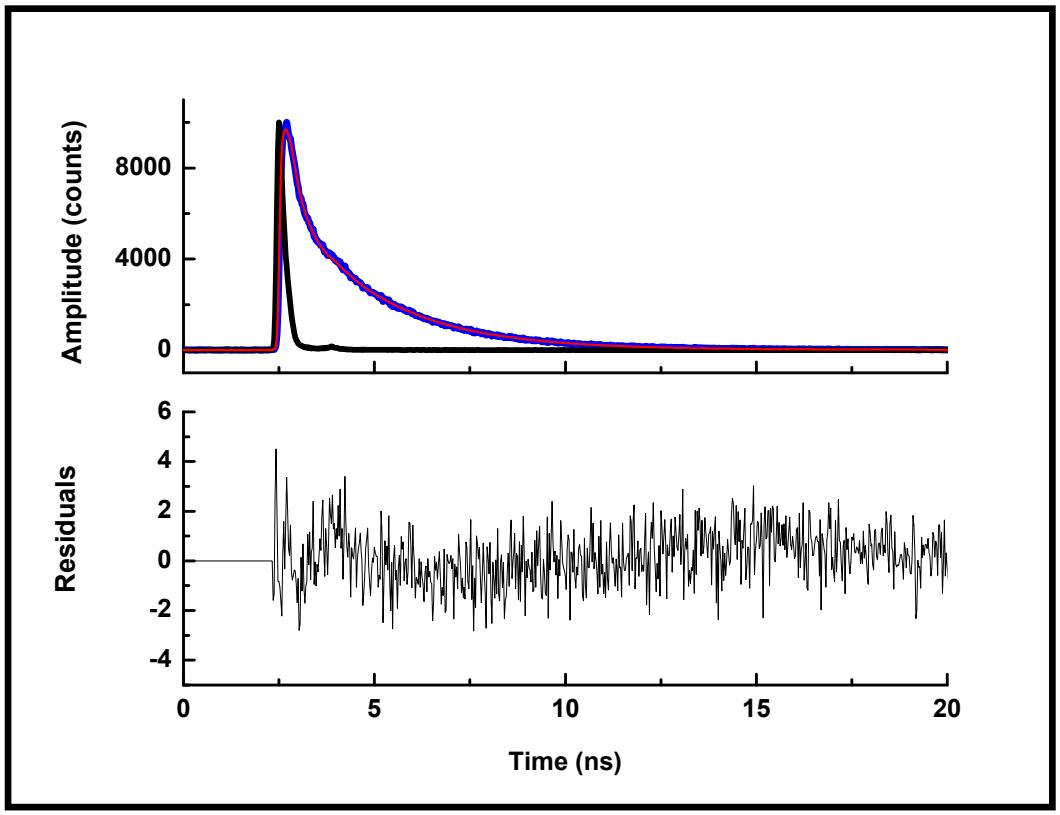

Figure 4.1: Fluorescence decay curve of **2**-SiNPs in DMSO.

4.2 Triplet quantum yields and lifetimes

Triplet quantum yield represents thefraction of the absorbing species that has undergone intersystem crossing. The absorbances of the phthalocyanines and phthalocyanine-silica nanoparticle conjugates were kept at approximately 1.5, at their maximum Q-band. After introduction of the solution into a 1 cm quartz cell, argon was bubbled into the solution for 15 min to remove oxygen. The triplet quantum yields were determined using equ.1.2. A high triplet quantum yield corresponds to low fluorescence quantum yield. The triplet quantum yields are listed in **Table 4.1.** A typical triplet decay curve is shown in **Figure 4.2**, with **1**-SiNPs used as an example. For the Pcs without SiNPs the largest ϕ_T was for **4** in DMSO at 0.89, lowest for **2** at 0.51. An increase in triplet quantum yield for **1**-SiNPs following doping was observed, the same was observed for **3**-SiNPs. Increase in ϕ_T values has been reported for encapsulated MPc complexes [**73**]. For complex **1**, the increase in ϕ_T value could be due to the higher loading,**Table 3.2**, though the high loading could also induce aggregation. It has also been reported the flat and rigid aromatic core of the phthalocyanine allows it to be trapped within the silica network [**85**]. Thus for unsubstituted (hence flat) complex **1**, it is possible the molecules stayed within the silica matrix hence resulting in improved ϕ_T value.Complex **3** has low loading but shows an increase in ϕ_T values, showing that it is not only the loading that affects the $\phi_T$values. It is possible that the electrostatic attraction between the positively charged Pc and the negatively charged SiNPs results in a stable conjugate and hence an increase in ϕ_T value. There was a decrease in triplet quantum yield for **2**-SiNPs. Complex **2** is neutral and not as flat as complex **1** due to the presence of amino phenoxy group. Thus complex **2** may not have been effectively trapped in

silica matrix, resulting in energy loses, hence a decrease in ϕ_T value. For **4**-SiNPs a slight decrease in ϕ_T value in DMSO was observed.

For chemically linked conjugate (**6**-SiNPs (linked)), the triplet quantum yield was higher compared to the doped conjugate (**6**-SiNPs(doped)), the latter was almost twice the chemically linked conjugate, **Table 4.1**. The decrease in triplet quantum yields for **6**-SiNPs (doped) could be due to non-radiative processes occurringwhen trapped within the matrix compared to the surface grafted chemically linked Pc in **6**-SiNPs (linked), since the loading is about the same. There could be energy losses due to interaction of Pc molecules within the matrix for **6**-SiNPs (doped). For complexes **5,7** and **8** the triplet quantum yields were not determined.

A decrease in triplet lifetimes is expected with an increase in triplet quantum yields and vice versa [**100**]. A decrease in triplet lifetimeswas observed for all conjugates, except for **4**-SiNPs where there was an elongation, which could be due to how the Pc is oriented in the SiNPs.

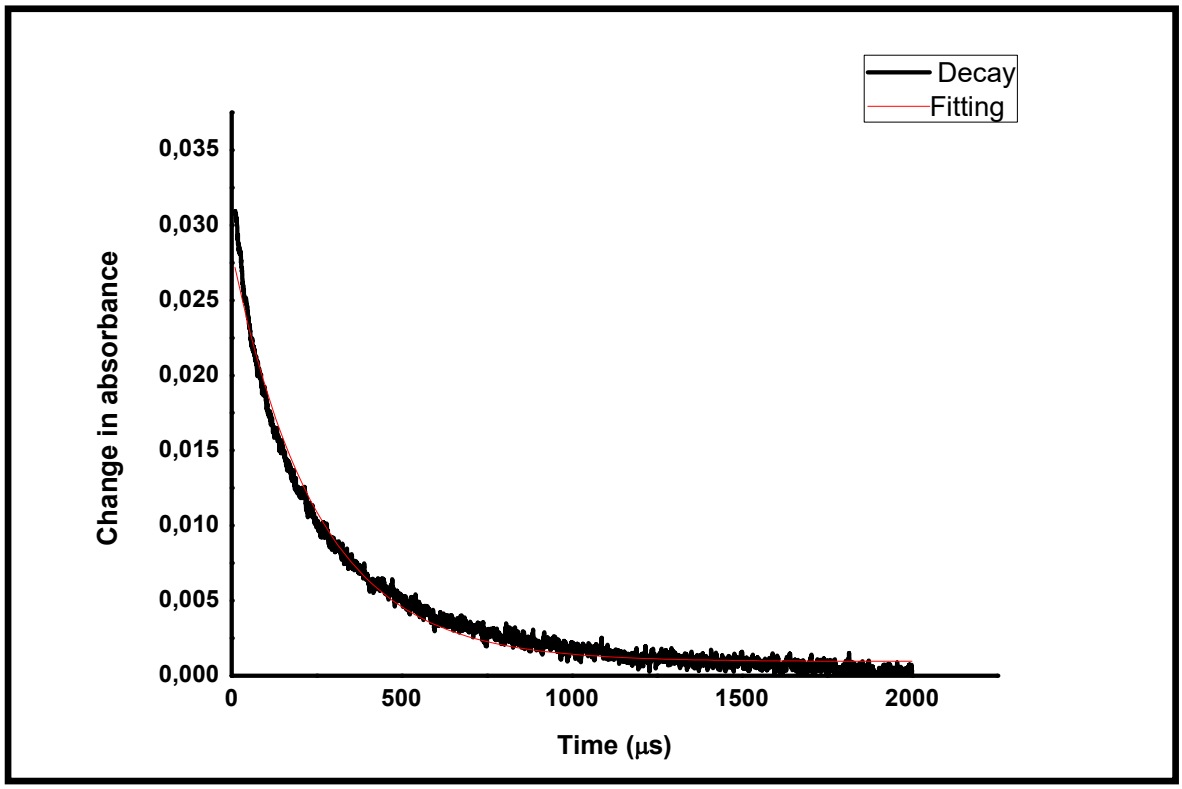

Figure 4.2: Triplet decay curve of **6** in DMSO.

4.3 Singlet oxygen quantum yields

Photosensitisers in their triplet state can transfer energy to ground state molecular oxygen andin that process singlet oxygen is produced. The production of singlet oxygen is highly dependent on triplet quantum yield, lifetime and the energy transfer efficiency of photosensitiser in its triplet excited state. DPBF was used as a singlet oxygen quencher in DMSO and ADMA as the quencher in water.The experiments were conducted at room temperature using 1.5 ml of each Pc or Pc-SiNP, or SubPcs mixed with equal volumes of ADMA or DPBF. Absorbance of the MPc, MPc-SiNPs, or SubPc was at 1.5 at the Q-band and for DPBF/ADMA absorbance was at 2. The absorbance profile of the DPBF is shown in **Figure 4.3** (using **6** as an example). A gradual decrease in the absorbance of DPBF was observed suggesting singlet

oxygen was produced, **Figure 4.3**. There were no decreases in the Q-band for both the MPcs and SubPcs, (as seen in **Figure 4.3** for MPcs), this therefore proves that theMPc was very stable during irradiation.It is expected that when ϕ_T values increase, ϕ_Δ values will also increase. Singlet oxygen quantum yield values are summarised in **Table 4.1**. Complex **4** had the largest singlet quantum yield, and **2**had the lowest in DMSO, which correspond to ϕ_T values discussed above. Complex **5** could not be compared to other MPcs since a different solvent was used.

An increase in singlet oxygen quantum value was obtained for **3**-SiNPs (in both DMSO:water and DMSO) was observed compared to **3**, the increase corresponds to the increase in triplet quantum yields of **3**-SiNPs. For **2**-SiNPs, there was a decrease in singlet oxygen quantum value compared to **2**, the decrease corresponds to the decrease in triplet quantum yields of **2**-SiNPs. For **1**-SiNPsthere was an increase in triplet quantum yield but a decrease in singlet oxygen quantum yield. Usually a decrease in singlet oxygen in the presence of NPs is associated with screening effect where NPs prevent oxygen molecules from interacting with excited triplet phthalocyanine [**101**]. The decrease for **1**-SiNPs could be because of the screening effect but it is not clear why this effect affects **1**-SiNPs only since the SiNPs conjugates are about the same size. There was also an increase in singlet oxygen quantum value for **4**-SiNPs in both DMSO and DMSO:water, even though there was a slight decrease in triplet quantum yield. Complex **4** is negatively charged and is most likely to be repelled by SiNPs due the negative hydroxide groups on the latter, hence may not suffer from the screening effect observed for **1**-SiNPs. A low singlet quantum yield for **5** in toluene was observed. There are many factors that contribute to the singlet quantum yield such as the solvent effect (viscosity and polarity), fluorescence quantum yields amongst others [**102-104**]. A large increase in the

singlet quantum yield was observed following conjugation, corresponding to the increase in triplet quantum yield for **6**-SiNPs (linked), however, the doped conjugate showed lower singlet quantum yield values compared to the chemically linked, showing no advantage of doping, ϕ_{Δ} value for **6**-SiNPs (doped) is less than that of **6** corresponding to the decrease in ϕ_T**.** A high singlet oxygen ϕ_{Δ} value for **8** was observed compared to **7** corresponding to the decrease in ϕ_F.

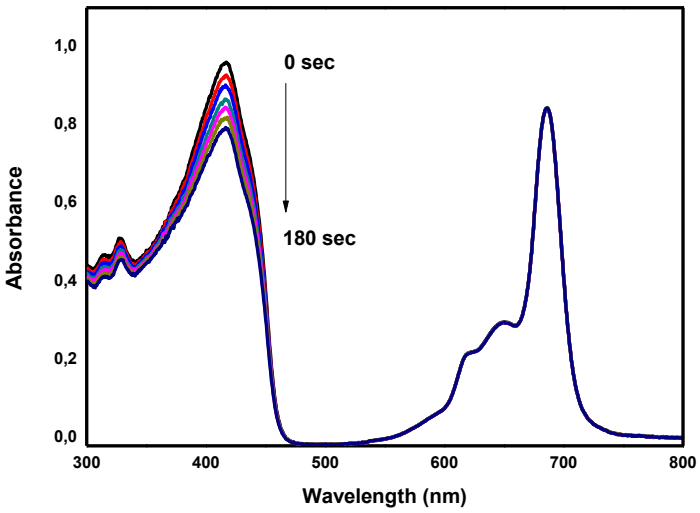

Figure 4.3: DPBF decay profile of **6**in DMSO.

4.4 Conclusions

*Physico-chemical properties of MPcs, MPc-SiNPs conjugates and SubPcs are reported. An improvement in the photophysical properties of some MPcs following conjugation/doping was observed. The singlet oxygen quantum yield of complex **4** was however lower than that of complex **1** but higher than for complexes **2** and **3** in DMSO. Following doping onto SiNPs, the singlet oxygen quantum yields increased for positively charged **3** and the negatively charged **4**, but not for complex **2**. **5** showed lower singlet quantum yields, but could not be*

*compared to other MPcs since the solvent used was different. There was no decrease in ϕ_{Δ} for **6**-SiNPs (doped) compared to **6**, however, for 6-SiNPs (linked) there was an improvement in both triplet and singlet quantum yields. SubPcs had high singlet oxygen values.*

Chapter Five
General conclusions

5.1 General conclusions

The syntheses and characterization of SiNPs doped with unsubstituted ZnPc (neutral, **1**), Zn tetraaminophenoxyphthalocyanine (neutral, **2**), tetrakis[4-(iodo-N-methylpyridinium)thio] phthalocyanine (cationic, **3**), Zn tetra sulfophenoxyphthalocyanine (anionic, **4**) and zinc tris[(4-(pyridin-4-ylthio)-2-thio-4-methylthiazol-5-yl)acetic acid phthalocyanine, (neutral, **6**) was successfully carried out. XPS, FTIR, EDX and other techniques were used to confirm the doping/conjugation of MPcs to SiNPs.

The ground state electronic behaviours of the conjugates were similar to those of MPcs alone. A slight enhancement around the B-region of the MPcs was observed due to the presence of SiNPs. There were slight decreases in fluorescence quantum yields for some SiNPs-MPcs conjugates compared to the MPcs alone, with no significant decrease in the fluorescence lifetimes. Singlet oxygen quantum yields improvement following doping was dependent on the nature of the MPc. Complex **6**, chemically linked MPc to SiNPs showed improvement in singlet oxygen quantum yield compared to physically linked MPc. Complex **7** showed an improvement in fluorescence and singlet oxygen quantum yield following axial ligand exchange (**8**).

5.2 Future

Doping/Conjugation MPcs to SiNPs has been proven to enhance the physic-chemical properties of MPcs. It would be interesting to study the antimicriobial properties of these MPc-SiNPs conjugates.

References

1. A. Braun, J. Tcherniac, Ber. Deut. Chem. Ges, 40 (**1907**) 2709.
2. C.C. Leznoff, A.B.P. Lever (Eds.), Phthalocyanines: Properties and Applications, Vols. 1-4; VCH Publishers (LSK) Ltd., Cambridge, (**1989**), (**1993**), (**1996**).
3. N.B. McKeown (Ed). Phthalocyanine Materials. Synthesis, Structure and Function; Cambridge University Press, Cambridge, (**1998**).
4. K.M. Kadish, K.M. Smith, R. Guillard (Eds.)The Porphyrin Handbook, Vol. 15; Academic Press, San Diego, (**2003**).
5. T.T. Tasso, Y. Yamasaki, T. Furuyama, N. Kobayashi, Dalt. Trans., 43 (**2014**) 5886.
6. L. Yuan, L. Gui, Y. Wang, Q. Zhang, L. Zhou, S. Wei, Spectrochim. Acta - Part A Mol. Biomol. Spectrosc., 158 (**2016**) 1.
7. E.T. Saka, C. Gol, M. Durmus, H. Kantekin, Z. Biyiklioglu, J. Photochem. Photobiol. A Chem., 241 (**2012**) 67.
8. M. Canlica, T. Nyokong, Dalt. Trans., 40 (**2011**) 1497.
9. M. Camerin, M. Moreno, M.J. Marin, C.L. Schofield, I. Chambrier, M.J. Cook, O. Coppellotti, G. Jori, D.A. Russell, Photochem. Photobiol. Sci., 15 (**2016**) 618.
10. H. Abramczyk, B. Brozek-Pluska, J. Surmacki, M. Tondusson, E. Freysz, J. Photochem. Photobiol. A Chem., 332 (**2017**) 10.
11. D. Dei, G. Chiti, M.P. De Filippis, L. Fantetti, F. Giuntini, M. Soncin, G. Jori, G. Roncucci, J. Porphyr Phthalocyanines, 10 (**2006**) 147.
12. O.J. Achadu, T. Nyokong, New J. Chem., 41 (**2017**) 1447.

13. N. Nwaji, D.O. Oluwole, J. Mack, M. Louzada, S. Khene, J. Britton, T. Nyokong, Dyes Pigm, 140 (**2017**) 417.
14. D. Sharma, A. Huijser, J. Savolainen, G. Steen, J.L. Herek, Faraday Discuss., 163 (**2013**) 433.
15. A. Meller, A.Ossko, Monatsh. Chem., 103 (**1972**) 150.
16. E. Ohno-Okumura, K. Sakamoto, T. Kato, T. Hatano, K. Fukui, T. Karatsu, A. Kitamura, T. Urano, Dyes Pigm, 53 (**2002**) 57.
17. H. Xu, D.K.P. Ng, Chem. - An Asian J., 4 (**2009**) 104.
18. W.M. Sharman, J.E. Van Lier,BioconjugateChem., 16 (**2005**) 1166.
19. B. Del Rey, U. Keller, T. Torres, G. Rojo, F. Agullo-Lopez, S. Nonell, C. Martí, S. Brasselet, I. Ledoux, J. Zyss, J. Am. Chem. Soc., 120 (**1998**) 12808.
20. K. Sakamoto, S. Yoshino, M. Takemoto, K. Sugaya, H. Kubo, T. Komoriya, S. Kamei, S. Furukawa, Am. J. Anal. Chem., 5 (**2014**) 1037.
21. L.C. Kasi Viswanath, L.D. Shirtcliff, S. Krishnan, N. V. Handa, K. Darrell Berlin, Tetrahedron Lett., 55 (**2014**) 4199.
22. N.B. Mckeown, J. Painter, J. mater. chem., 4 (**1994**) 1153.
23. I. Ozcesmeci, A. Tekin, A. Gul, Synth. Met., 189 (**2014**) 100.
24. N. Nombona, E. Antunes, C. Litwinski, T. Nyokong, Dalt. Trans., 40 (**2011**) 11876.
25. D. Gonzalez-rodriguez, C.G. Claessens, T. Torres,J. Porphyr Phthalocyanines, 13 (**2009**) 203.
26. K.J. McAuliffe, M.A. Kaster, R.G. Szlag, E.R. Trivedi, Int. J. Mol. Sci., 18 (**2017**) 1177.
27. J. Guilleme, L. Martinez-fernandez, D. Gonzalez-, I. Corral, M. Yanez, T. Torres, J. Guilleme, L.M.- Fernandez, D.G.- Rodriguez, I. Corral, J. Am.

Chem. Soc., 136 (**2014**) 14289.

28. S. Shimizu, N. Kobayashi, Chem. Commun., 50 (**2014**) 6949.
29. M. Gouterman, In The Porphyrins,(Ed. D.Dolphin), Part A, Physical Chemistry, Academic Press, New York, (**1978**), pp. 1–159.
30. A. J. McHugh, M. Gouterman, Theor. Chim. Acta, (**1987**) 246.
31. A.M. Schaffer, M. Gouterman, E.R. Davidson, Theor. Chim. Acta, 30 (1973) 9.
32. M.B. Spesia, E.N. Durantini,FEMS Immunology and Medical Microbiology, 44 (**2005**) 289.
33. A. Lyubimtsev, Z. Iqbal, G. Crucius, S. Syrbu, E.S. Taraymovich, T. Ziegler, M. Hanack, J. Porphyr. Phthalocyanines, 15 (**2011**) 39.
34. R.Z.U. Kobak, M.U. Ari, A. Tekin, A. Gul, Chem. Phys., 448 (**2015**) 91.
35. P.J. Camp, A.C. Jones, R.K. Neely, N.M. Speirs, J. Phys. Chem. A, 106 (**2002**) 10725.
36. X. Zhang, H. Xu, J. chem. soc. faraday trans., 89 (**1993**) 3347.
37. G. Weber, F.W.J. Teale, Trans. Faraday Soc., 53 (**1957**) 646.
38. A. Ogunsipe, D. Maree, T. Nyokong, J. Mol. Struct., 650 (**2003**) 131.
39. P. G. Seybold, M. Gouterman, Photochem. Photobiol., (**1969**) 229.
40. D. M, Mafukidze, T. Nyokong,Journal Coord. Chem., 21 (**2017**) 3598.
41. S.M. Bachilo, R.B. Weisman, J. Phys. Chem. A, 104 (**2000**) 7711.
42. S. Reindl, A. Penzkofer, Chemical Physics, 213 (**1996**) 429.
43. B. Amand, R. Bensasson,ChemicalPhysics letters, 34 (**1975**) 44.
44. T.H. Tran-Thi, C. Desforge, C. Thiec, S. Gaspard, J. Phys. Chem., 93 (**1989**) 1226.
45. N. Njemuwa, Jones. B, Mack. J, Oluwole.D.O, Nyokong.T, J. PhotochemPhotobiolA: Chemistry 346 (**2017**) 46

46. W. Spiller, H. Kliesch, D. Wohrle, S. Hackbarth, B. Roder,G. Schnurpfeil, J. Porphyr Phthalocyanines, 2 (**1998**) 145.
47. T. Nyokong, E. Antunes, In Chapter title: *Photochemical and photophysical properties of metallophthalocyanines: The Handbook of Porphyrin Science*. Eds. Kadish, K. M.; Smith, K. M.; Guilard, R. Vol.7, chapt. 34 pp247-349, World Scientific, Singapore, (**2010)**.
48. P.Gottschalk,J.Paczkowski,D. C. Neckers, J. Photochem, 35 (**1986**) 277.
49. O. Tsaryova, A. Semioshkin, D. Wohrle, V.I. Bregadze, J. Porphyr Phthalocyanines, 9 (**2005**) 268.
50. M. Ganschow, D. Worhle, G. Schulz-Ekloff, J. Porphyr Phthalocyanines, 3 (**1999**) 299.
51. B. Agboola, K.I. Ozoemena, T. Nyokong, Electrochim. Acta, 51 (**2006**) 4379.
52. B. Marydasan, A.K. Nair, D. Ramaiah, J. Phys. Chem. B, 117 (**2013**) 13515.
53. W. Chidawanyika, T. Nyokong, J. Photochem. Photobiol. A Chem., 206 (**2009**) 169.
54. A. Skripchenko, S. J. Wagner, D. Thompson-Montgomery, H. Awatefe, Transfusion, 46 (**2006**) 213.
55. U. Demirbas, C. Gol, B. Barut, R. Bayrak, M. Durmus, H. Kantekin, İ. Degirmencioglu, J. Mol. Struct., 1130 (**2017**) 677.
56. P. Khoza, E. Antunes, T. Nyokong, Polyhedron, 61 (**2013**) 119.
57. A. Nas, G. Dilber, M. Durmus, H. Kantekin, Spectrochim. Acta - Part A Mol. Biomol. Spectrosc., 135 (**2015**) 55.
58. R.P. Bagwe, C. Yang, L.R. Hilliard, W. Tan, Langmuir, 20 (**2004**) 8336.
59. N. Rapulenyane, E. Antunes, T. Nyokong, New J. Chem., 37 (**2013**) 1216.

60. Z. Xie, H. Gong, M. Liu, H. Zhu, H. Sun, J. Biomater. Sci. Polym. Ed., 27 (**2016**) 55.
61. Y. Zhang, Z. Zhi, T. Jiang, J. Zhang, Z. Wang, S. Wang, J. Control. Release, 145 (**2010**) 257.
62. I.I. Slowing, B.G. Trewyn, S. Giri, V.S.Y. Lin, Adv. Funct. Mater., 17 (**2007**) 1225.
63. I. Roy, T.Y. Ohulchanskyy, H.E. Pudavar, E.J. Bergey, A.R. Oseroff, J. Morgan, T.J. Dougherty, P.N. Prasad, J. Am. Chem. Soc., 125 (**2003**) 7860.
64. W. Stober, A. Fink, E. Bohn, J. Colloid Interface Sci., 26 (**1968**) 62.
65. M. Montalti, L. Prodi, N. Zaccheroni, G. Battistini, S. Marcuz, F. Mancin, E. Rampazzo, U. Tonellato, Langmuir, 22 (**2006**) 5877.
66. K. Nozawa, H. Gailhanou, L. Raison, P. Panizza, H. Ushiki, E. Sellier, J.P. Delville, M.H. Delville, Langmuir, 21 (**2005**) 1516.
67. K.S. Finnie, J.R. Bartlett, C.J.A. Barbe, L. Kong, Langmuir, 23 (**2007**) 3017.
68. D.O. Oluwole, T. Nyokong, Dyes Pigm, 136 (**2017**) 262.
69. C. Argyo, V. Weiss, C. Brauchle, T. Bein, Chem. Mater. 26 (**2014**) 435.
70. Q. He, J. Shi, J. Mater. Chem., 21 (**2011**) 5845.
71. A.A. Voronina, I.A. Tarasyuk, Y.S. Marfin, A.S. Vashurin, E. V. Rumyantsev, S.G. Pukhovskaya, J. Non. Cryst. Solids, 406 (**2014**) 5.
72. R. Lin, L. Zhou, Y. Lin, A. Wang, J.H. Zhou, S.H. Wei, Spectroscopy, 26 (**2011**) 179.
73. A. Fashina, E. Amuhaya, T. Nyokong, Spectrochim. Acta - Part A Mol. Biomol. Spectrosc., 137 (**2015**) 294.
74. A. Fashina, E. Antunes, T. Nyokong, New J. Chem., 37 (**2013**) 2800.

75. A. Fashina, E. Antunes, T. Nyokong,J. Porphyr Phthalocyanines, 18 (**2014**) 396.

76. S. Moeno, E. Antunes, S. Khene, C. Litwinski, T. Nyokong, Dalt. Trans., 39 (**2010**) 3460

77. Y. Takagi, K. Ohta, S. Shimosugi, T. Fujiia, E. Itoh, J. Mater. Chem., 22 (**2012**) 14418

78. M. Ambroz, A. Beeby, A. J. MacRobert, M. S. C. Simpson, R. K. Svensen, D. Phillips, J. Photochem. Photobiol. B, 9 (**1991**) 87

79. V.Malingam, S.Onelin, M. Peter, B.J.Ravoo, J. Huskens, D.B, Rein-Houdt,Langmuir, 20 (**2004**) 11756.

80. N. Masilela, T. Nyokong, J.Photochem. Photobio A: Chem,. 223 (**2011**) 124

81. B. Gorji, M.R. AllahgholiGhasri, R. Fazaeli , N. Niksirat, J. Appl. Chem. Res., 6 (**2012**) 22.

82. K. Yoncheva, M. Popov , A. Szegedi , J. Mihaly , B. Tzankov, N. Lambov, S. Konstantinov, V. Tzankova, F. Pessina, M. Valoti, Journal of Solid State Chemistry, 211 (**2014**) 154.

83. M.J. Stillman, T. Nyokong, Phthalocyanines - Properties and Applications, in: A.B.P. Lever, C.C. Leznoff (Eds.) Volume 1, New York, (**1989**).

84. C. G. Claessens, D. Gonzalez-Rodrıguez, T. Torres, Chem. Rev., 102 (**2002**) 835.

85. A. K. Eckert, M. S. Rodrıguez-Morgade, T. Torres, Chem. Commun., (**2007**) 4104.

86. A. Auger, J. Samuel, O. Poncelet, O. Raccurt, NanoscaleRes. Lett., *6* (**2011**) 328.

87. E. Secret, M. Maynadier, A. Gallud, M. Gary-Bobo, A. Chaix, E. Belamie, P. Maillard, M.J. Sailor, M. Garcia, O. Durand, F. Cunin ,J.Chem. Commun. 49 (**2013**) 202.
88. O. Hocine, M. Gary-Bobo, D. Brevet, M. Maynadier, S. Fontanel, S. Raehm, S. Richeter, B. Loock, P. Couleaud, C. Frochot, C. Charnay, G. Derrien, M. Smaihi, A. Sahmoune, A. Morere, P. Maillard, M. Garcia, J.O. Durand,J. Pharm., 402 (**2010**) 22.
89. A.V. Zasedatelev, T.V. Dubinina, D.M. Krichevsky, V.I. Krasovskii, V.Y. Gak, V.E. Pushkarev, L.G. Tomilova, A.A. Chistyakov, J. Phys. Chem*. C*, 120 (**2016**) 1816
90. K. Natte, T. Behnke, G. Orts-Gil, C. Wurth, J.F. Friedrich, W. Osterle, U. Resch-Genger, Alexa dyes,J. Nano. Part.Res, 14 (**2012**) 680
91. S. Xu, S. Hartvickson, J.X. Zhao,ACS Appl. Mater. Interfaces, 3 (**2011**) 1865.
92. R. Prabakaran, R. Kesavamoorthy, G.L.N. Reddy, F.P. Xavier, Phys Status Solid, 229 (**2002**), 1175.
93. P. Borker, A.V. Stalker, Indian. J. Chemical Technology, 13 (**2006**) 341.
94. O.R. Ogbodu, T. Nyokong, J. Photochem. Photobiology A: Chemistry, 274 (**2014**) 83.
95. X.F. Zhang, X. Li, L. Niu, L. Sun, L. Liu,J. Fluoresc., 19 (**2009**) 947.
96. R. Mayildurai , G. Dhinakaran , S. Karthikeyan, R. Ashokkumar, Rasayan.J.Chem, 10 (**2017**) 1242
97. S. Bonacchi, D. Genovese, R. Juris, M. Montalti, L. Prodi,E. Rampazzo, M. Sgarzi, N. Zaccheroni, Top. Curr. Chem. 300 (**2011**) 93.
98. J.R. Darwent, I. McCubbin, D. Phillips, Faraday Trans., 78 (**1982**) 347.
99. O. Goktuga , C. Golb, M. Durmus, J. PorphyrPhthalocyanines, 21 (**2017**) 539.

100.S,Tobita, K. Ida, K. Shiobara,Res. Chem. Intermed.,27 (**2001**) 205.

101.E.I. Sagun, E.I. Zenkevich, V.N. Knyukshuto, A.M. Shulga, D.A. Starukhin, C. von Borczyskowski, Chem. Phys. 275 (**2002**) 211.

102.P.R. Ogilby, C.S. Foote, J. Am. Chem. SOC., 105 (**1983**) 3423.

103.R.W. Redmond, S.E. Braslavsky, Chemical physics letters, 148 (**1988**) 523

104.J.H. Ha, M.S. Kim, Y. Park, S.Ryu, M. Park, K. Shin, Y.R. Kim, Bull. Korean. Chem. Soc., 23 (**2002**) 281.